CO2-SO2 clathrate hydrate formation on early Mars

Eric Chassefière, Emmanuel Dartois, Jean-Michel Herri, Feng Tian, Frédéric Schmidt, Olivier Mousis, Azzedine Lakhlifi

CO_2-SO_2 clathrate hydrate formation on early Mars

Eric Chassefière[a,b], Emmanuel Dartois[c], Jean-Michel Herri[d], Feng Tian[e], Frédéric Schmidt[a,b], Olivier Mousis[f,g], Azzedine Lakhlifi[f]

[a] Univ Paris-Sud, Laboratoire IDES, UMR8148, Université Paris-Sud, Bât. 504, Orsay, F-91405, France;

[b] CNRS, Orsay, F-91405, France.

[c] IAS, Université Paris-Sud, CNRS, France

[d]Centre SPIN , ENS des Mines de Saint-Etienne, France

[e]Center for Earth System Sciences, Tsinghua University, Beijing, China

[f]Institut UTINAM, UMR 6213, Université de Franche-Comté & OSU THETA de Franche-Comté, France

[g]Université de Toulouse; UPS-OMP; CNRS-INSU; IRAP; 14 Avenue Edouard Belin, 31400 Toulouse, France

Corresponding author

Eric Chassefière

IDES, Univ. Paris-Sud, CNRS

Tel : 33 1 69 15 67 48

Fax : 33 1 69 15 49 11

E-mail : eric.chassefiere@u-psud.fr

Second revised version submitted to Icarus

Abstract

It is generally agreed that a dense CO_2-dominant atmosphere was necessary in order to keep early Mars warm and wet. However, current models have not been able to produce surface temperature higher than the freezing point of water. Most sulfate minerals discovered on Mars are dated no earlier than the Hesperian, despite likely much stronger volcanic activities and more substantial release of sulfur-bearing gases into Martian atmosphere during the Noachian. Here we show, using a 1-D radiative-convective-photochemical model, that clathrate formation during the Noachian would have buffered the atmospheric CO_2 pressure of early Mars at ~2 bar and maintained a global average surface temperature ~230 K. Because clathrates trap SO_2 more favorably than CO_2, all volcanically outgassed sulfur would have been trapped in Noachian Mars cryosphere, preventing a significant formation of sulfate minerals during the Noachian and inhibiting carbonates from forming at the surface in acidic water resulting from the local melting of the SO_2-rich cryosphere. The massive formation of sulfate minerals at the surface of Mars during the Hesperian could be the consequence of a drop of the CO_2 pressure below a 2-bar threshold value at the late Noachian-Hesperian transition, which would have released sulfur gases into the atmosphere from both the Noachian sulfur-rich cryosphere and still active Tharsis volcanism. A lower value of the pressure threshold, down to ~0.5 bar, could have been sufficient to maintain middle and high latitude regions below the clathrate formation temperature during the Noachian and to make the trapping of SO_2 in clathrates efficient. Our hypothesis could allow to explain the formation of chaotic terrains and outflow channels, and the occurrence of episodic warm episodes facilitated by the release of SO_2 to the atmosphere. These episodes could explain the formation of valley networks and the degradation of impact craters, but remain to be confirmed by further modeling.

Key words : Early Mars, CO_2, SO_2, clathrates, sulfates, cryosphere, carbonates**.**

1. Introduction

Sulfur dioxide (SO_2) has been proposed as a possible greenhouse gas which worked together with CO_2 to raise the surface temperature of early Mars above the freezing point of water (Halevy et al., 2007; Johnson et al., 2008; Postawko and Kuhn, 1986), allowing liquid water to flow at the surface of the planet and carving the presently observed valley networks and outflow channels. However, the cooling from sulfur gases as a result of sulfate aerosol formation is an observational fact for the current atmosphere of Earth. On early Mars, the cooling effect of sulfate aerosols would also have counteracted efficiently the warming effect due to SO_2 greenhouse effect and sulfur outgassing. After a short period of warming, the presence of sulfate aerosols would have resulted in a colder surface, with a net cooling, instead of warming, of the planet (Tian et al., 2010). No mechanism to keep ancient Mars warm and wet through greenhouse effect has been generally accepted so far, suggesting a cold and wet early Mars. Much of the aqueous activity on Mars could have occurred in subsurface hydrothermal systems powered by magmatic or impact activity (Squyres and Kasting, 1994; Griffith and Shock, 1995; Segura et al., 2002; 2008), rather than at the surface of the planet.

Sulfur, under both oxidized (SO_2) and reduced (H_2S) forms, could have been released in large amount by volcanism during the Noachian. From several hundred millibar to around one bar of sulfur could have been outgassed along Martian history, most of which during the Noachian and the Hesperian (see e.g. Craddock and Greeley, 2009; Gaillard and Scaillet, 2009). The reconstructed evolution of the cumulated amount of released SO_2 since the early Noachian, shortly after accretion, is shown in Figure 1. It has been derived from both the CO_2 volcanic release rates calculated from a thermo-chemical evolution model of Mars (Grott et al., 2011) and a photogeological analysis of the Martian surface (Craddock and Greeley, 2009, referred to as CG09 in this paper). The ratio between SO_2 and CO_2 molar fractions in the

Fig.1

volcanic gas f_{SO2}/f_{CO2} is typically in the range from 0.5 to ~1 (see Fig. 5 in Gaillard and Scaillet, 2009). The evolutions of the CO_2 partial pressure (denoted by p_{CO2} in the following) for two values (0.01 and 1) of the surface fraction covered by hot upwellings (f_p) are plotted on Figure 4b in Grott et al. (2011). By applying the ratio f_{SO2}/f_{CO2} to Grott et al. curves, and taking into account the difference of molar mass between CO_2 (44 g/mol) and SO_2 (64 g/mol), we have plotted in Fig. 1 the corresponding evolutions of the cumulated amount of outgassed SO_2, expressed in pressure units, and the corresponding global equivalent layer (GEL) thickness of the sulfate mineral assuming that all the released sulfur is involved in anhydrite formation. The other plotted curve is obtained from a photogeological analysis of the Martian surface yielding a cumulated lava extrusion volume of 0.7×10^8 km^3 (CG09), by assuming that basalts contain 7000 ppm sulfur by mass (an upper range according to Gaillard and Scaillet, 2009), that is 10 times more than assumed in CG09. This curve would be ~3 times lower assuming a lower range of 2500 ppm of S and 4 times higher assuming a lava extrusion volume of 3×10^8 km^3 (Gaillard and Scaillet, 2009). Both models and observations therefore suggest a cumulated pressure of outgassed SO_2 of typically ~1 bar, corresponding to a ~40 m thick sulfate GEL, within a factor of 3 both ways.

Interestingly, all sulfate minerals detected at the surface of Mars by OMEGA/Mars Express have been emplaced during the Hesperian, a relatively late epoch in Martian history (Bibring et al., 2006). Later observations of CRISM on MRO have revealed additional sulfate deposits, a few of them under the form of interbedded phyllosilicate and sulfate layers in sediments of Noachian craters (Terra Sirenum) in the Southern hemisphere (Murchie et al., 2009). These intracrater deposits are relatively widespread, far from those mapped by OMEGA and at higher elevation, excluding that they have been transported from equatorial regions (Wray et al., 2011). Although a younger age for these sediments cannot be excluded, they are suspected to have formed by evaporitic processes in an acidic context at the Noachian. Such formations

associating phyllosilicates and sulfates are also found in terrestrial acidic saline lake deposits (Baldridge et al., 2009). Most of sulfate deposits are observed in Hesperian terrains. They consist of several kinds of formations: (i) Hesperian layered sulfates under the form of extended deposits in Terra Meridiani, (ii) Interior Layered Deposits (ILD) throughout the Valles Marineris trough system consisting of massive mounds of layered material up to several kilometers thick, (iii) gypsum deposits in north polar dune field (Gaillard et al., 2012). Sulfur is also part of soil and dust at the global scale at an average level of ~6.8 % (King and McLennan, 2010). It has been suggested that some sulfates could have been formed by evaporitic processes in the Valles Marineris region prior to Tharsis formation, then redistributed by fluvial transport to Meridiani Planum, where they are now observed, during the elevation of the Tharsis uplift (Fan et al., 2008). If so, sulfates detected in Hesperian terrains could have been formed in the Noachian. The question of the origin of sulfates is debated, and at least some of the observed deposits could have formed in the late Noachian. In the present paper, we make the hypothesis that most of the sulfates observed in equatorial regions (layered deposits, ILD) have been formed at the Hesperian (not excluding a start at the late Noachian), and propose an explanation for the scarcity of sulfates in Noachian terrains, and their apparently massive deposition at the Hesperian.

The evolution of CO_2 on Mars is poorly constrained. Despite the discovery of carbonates in SNC meteorites and the recent orbital and in situ observations of carbonate rocks at some locations on the surface of Mars (see e.g. Niles et al., 2012), carbonates are not proved to be extensively present on Mars. The lack of global carbonate outcrops on Mars, which seems to contradict a massive presence of CO_2 in its early atmosphere, could be explained by either the action of sulfuric or sulfurous acids in large, standing bodies of water suppressing the formation of carbonates (Fairen et al., 2004; Halevy et al., 2007), or a rapid escape of early Martian CO_2 atmosphere (Tian et al. 2009, referred to as T09 in this paper), or both.

According to an early Mars upper atmosphere model (T09), the timescale for 1 bar of CO_2 to be removed through thermal escape would have been ~1 Myr at 4.5 billion years ago (Ga) and ~10 Myr at 4.1 Ga. Note that at first stages, during typically the first hundred million years, carbon escape may have been slowed down by water hydrodynamic escape, which is not taken into account in T09. If Mars was endowed with amounts of CO_2 similar to those found on Venus and the Earth (~100 bar), and according to the model of T09, most of its initial CO_2 inventory would have been lost within the first 100 Myr after its formation. A mechanism that can possibly help Mars to keep its CO_2 inventory is carbonate formation through weathering of basalt (Pollack et al. 1987). The same authors proposed that a dense CO_2 atmosphere (1 to 5 bar) could have been maintained during the Noachian by constant recycling of CO_2 back into the atmosphere through rapid burial and thermal decomposition of carbonate minerals. They calculated a typical cycling time of CO_2 at 273 K of ~10 Myr, decreasing to ~1 Myr at larger temperatures of 300 K for a CO_2 pressure of 1 bar, a temperature easily achievable in the subsurface even if the surface was cold. If the formation of carbonate through weathering has occurred at a rate comparable to that of carbon thermal escape, substantial amounts of carbon could have been trapped in the format of carbonates and cycled through the subsurface-hydrosphere-atmosphere system. If so, a significant atmosphere of CO_2 could have survived until 4.1 Ga. The combination of a rapid formation of carbonate and a rapid thermal escape of carbon on Noachian Mars could have decreased the atmospheric pressure of Noachian Mars even more rapidly, resulting in shorter warm periods and longer, more frequent cold periods on Noachian Mars. It is important to note that the timescales of carbonate formation and their further destabilization are still poorly understood.

The present inventory of water on Mars is also poorly constrained. The total water content of the two perennial polar caps corresponds to a GEL of 16 m depth (Smith et al., 2001), and the

ice deposits sequestered in the Dorsa Argentea Formation (DAF), near the south polar cap, could have represented a ~15 m thick GEL in the past (Head and Pratt, 2001). Nevertheless, only a fraction of the initial water could remain today in DAF reservoir, corresponding to a ~5-7.5 m thick GEL. Other reservoirs, expected to have been active during late Amazonian, could be present in tropical and mid-latitude regions (Head and Marchant, 2009). But they probably represent only a minor contribution to the global reservoir. The total inventory of the known reservoir, including near-surface stores that are distributed across middle to high latitudes, has been estimated to correspond to a 35 m thick GEL (Christensen, 2006). The mega-regolith capacity is large, with up to a ~500 m thick GEL potentially trapped in the cryosphere, and hypothetically several additional hundreds of meters GEL (up to ~500 m) of ground water surviving at depth below the cryosphere (Clifford et al., 2010). It has been suggested that most of ground ice has been lost by sublimation at low latitudes, and that only small amounts of groundwater would survive today (Grimm and Painter, 2009), with therefore less water in the megaregolith. A ~500 m thick GEL is generally assumed to be required to explain the formation of outflow channels (Carr, 1987), and most of this water could be trapped today as water ice, and possibly deep liquid water, in the subsurface, as well as in subsurface hydrated minerals. Based on an analysis of the present Mars' atmospheric D/H ratio, it has been suggested that a water GEL of up to ~300-400 m depth could have been stored in crustal serpentine since the late Noachian due to hydrothermalism triggered by magmatic activity (Chassefière and Leblanc, 2011b).

In the present paper, we suggest that the formation of CO_2-SO_2 clathrate hydrates (indifferently written "clathrate hydrates" or "clathrates" in this article) in a potentially CO_2-dominant (a few bar) early atmosphere of Mars should have significantly decreased the atmospheric SO_2 and CO_2 contents and should have caused subsequent sulfur enrichment in early Mars cryosphere. As shown hereafter, for a CO_2 pressure above 2 bar, all volcanically

183 released SO_2 and the fraction of atmospheric CO_2 in excess of 2 bar should have been
184 converted to CO_2-SO_2 clathrates. In this way, the formation of sulfate particles in the
185 atmosphere could have been inhibited and there would have been neither long term net
186 cooling nor net warming from volcanic SO_2 eruptions. If atmospheric CO_2 pressure is
187 between 1 and 2 bar, we show that a fraction of volcanically released SO_2 would have been
188 converted to sulfate particles while the rest would have been trapped in clathrates. This
189 mechanism would have resulted in a stabilization of the surface temperature at the clathrate
190 equilibrium temperature after large volcanic events. At some time in the past, when the CO_2
191 pressure dropped below 1 bar, the formation of clathrates would have been totally inhibited
192 and the sulfur injected by volcanism into the atmosphere would have been fully converted
193 into atmospheric sulfate aerosols. Thus formation of sulfate minerals at the surface no earlier
194 than at the Hesperian could be explained by a decrease in atmospheric CO_2 pressure below
195 the 2 bar level occurring close to the late Noachian/ Hesperian transition.
196
197 In the following section, we describe the potential impact of CO_2-SO_2 clathrate formation on
198 the sulfur content in the atmosphere and the surface temperature. Then, we present an
199 extrapolation to low temperature of the thermodynamic properties of CO_2-SO_2 clathrates.
200 New calculations of the surface temperature of Mars in presence of sulfate particles for
201 different values of the CO_2 pressure are made, and consequences on the climate of early Mars
202 examined. After an assessment of the consequences of the presence of SO_2 on the trapping of
203 noble gases in clathrates, we discuss the possible implications of the present results and
204 measurements to be done by future missions to improve our understanding of the impact of
205 sulfur on early Mars' climate.
206

207 2. Formation of CO_2-SO_2 clathrate hydrate at high CO_2 pressure and SO_2 208 mixing ratio

The cooling effect of sulfate aerosols on the early Mars climate has been recently pointed out through a detailed 1-D photochemical/microphysical model of ancient Mars' atmosphere (Tian et al. 2010, referred to as T10 in this paper). Under certain CO_2 pressure, the surface temperature increases only slightly with enhanced level of atmospheric SO_2 at first because of the greenhouse contribution from SO_2. At atmospheric SO_2 concentration which could lead to meaningful surface warming, photochemistry processes induce the formation of sulfate aerosols which can reflect sunlight and cause surface cooling. The surface temperature for various SO_2 mixing ratios (T10) together with the equilibrium temperature of CO_2 clathrate hydrate (Mousis et al., 2012), and CO_2 ice, are plotted in Figure 2 as a function of the CO_2 pressure. At 3 bar atmospheric pressure and for a SO_2 mixing ratio of 10 ppmv, the amplitude of the cooling by sulfate aerosols is about 60 K (T10), resulting in a surface temperature low enough to allow the formation of CO_2 clathrate hydrates (and even CO_2 ice). For a lower SO_2 mixing ratio of 1 ppmv the cooling is smaller, of the order of 20 K, but sufficient to fall in the domain of stability of CO_2 clathrates (but not of CO_2 ice). Fig. 2

First, in a regime without sulfur, CO_2 clathrates are stable for p_{CO2}>2 bar due to the cooling effect of the Rayleigh scattering (T10). As a consequence any CO_2 pressure in excess of 2 bar results in the formation of CO_2 clathrate hydrates until the atmospheric CO_2 pressure is reduced to ~2 bar, with a stabilization of p/T values close to 2 bar/230 K. Thus, the atmospheric CO_2 pressure could have been maintained at ~2 bar during most of the Noachian, if atmospheric escape is neglected. Because carbon escaped rapidly during the early Noachian, this regime is possible only if a few bar of carbon sequestered first in crustal carbonates was recycled to the atmosphere by volcanism during the Noachian, since the amount of carbon released from the mantle to the atmosphere during the late Noachian and at later epochs is rather modest, a few hundreds millibar according to existing models (Grott et

al., 2011). The warming effect of CO_2 clouds by reflection of the IR radiation emitted by the surface (Forget and Pierrehumbert, 1997) is not taken into account in this simulation. At p_{CO2}=2 bar, the presence of CO_2 clouds may result in a surface temperature increase by ~5 K (Colaprete and Toon, 2003), somewhat increasing the temperature and pressure thresholds for the formation of CO_2 clathrates. Also, 1-D modeling provides only global average values and the local conditions may differ significantly from the average case. Formation of clathrates is expected to be more efficient in cold regions (polar caps) than at middle or lower latitudes. The possibility that a part of the CO_2 inventory may be stored under the form of clathrates has no significant impact on the discussion made in the previous section relative to the role of thermal escape. Indeed, any later decrease of the atmospheric CO_2 content following thermal escape would have resulted in the destabilization of CO_2 clathrates and a transfer to the atmosphere of an amount of CO_2 equal to that removed to space. In this regime, the CO_2 is buffering pressure and temperature around 2 bar/230 K until the total volatile CO_2 reservoir (ice, clathrate, and the atmosphere combined) decreased below 2 bar.

Second, the sporadic addition of SO_2 in the atmosphere by volcanic events into the previous regime would have had the following effects: (i) initial increase of the surface temperature by direct greenhouse effect, (2) rapid decrease of the surface temperature by formation of sulfate aerosols, in some cases below the equilibrium temperature of CO_2 clathrates (cf Fig. 2). If the atmospheric SO_2, which is the source of sulfate aerosols, was trapped together with CO_2 in clathrates hydrates, the SO_2 atmospheric content would have been decreased, which would have slowed down or even inhibited the formation of sulfate aerosols and the subsequent cooling. Through this mechanism, the atmospheric mixing ratio of SO_2, following volcanic events, will stabilize close to the mixing ratio maintaining a surface temperature equal the CO_2-SO_2 clathrate equilibrium temperature. As an example, for p_{CO2} = 3 bar, this equilibrium mixing ratio is of the order of 0.1 ppm (Fig. 2). Any increase of the atmospheric SO_2 mixing

ratio above this equilibrium value would have resulted in aerosol formation, cooling of the surface, formation of clathrates, and the removal of the remaining fraction of SO_2 gas from the atmosphere to clathrates. The higher the SO_2/CO_2 mixing ratio in the clathrates with respect to the gas, the more efficient this mechanism. If SO_2 is enriched with respect to CO_2 in the clathrates, formation of CO_2-SO_2 clathrates results in a decrease of the atmospheric SO_2 mixing ratio. If SO_2 is depleted in the solid phase, clathration results in an enrichment of SO_2 in the atmosphere. As shown in the next section, SO_2 is enriched by a factor of ~100-500 in the clathrate phase at ~220 K. The condensation of only 1% (or less) of the atmospheric CO_2 in clathrates, with therefore no significant change in p,T conditions, would have resulted in the removal of most atmospheric SO_2 to the cryosphere, implying that the proposed mechanism is highly efficient. Thus, once the regime described in the last paragraph is reached at p_{CO2} = 2 bar / 230 K, any addition of atmospheric sulfur will be incorporated into CO_2-SO_2 clathrates.

The goal of the next section is to study the composition of CO_2-SO_2 clathrates as a function of gas composition, in particular the SO_2/CO_2 mixing ratio in the clathrate as a function of the gas mixing ratio to estimate the efficiency of CO_2-SO_2 clathrate formation in transferring SO_2 from the atmosphere to the cryosphere.

3. Thermodynamic modeling of CO_2-SO_2 clathrates in Martian atmospheric conditions

3.1 Thermodynamical approach

The van der Waals and Platteeuw (1959) model describes the equilibrium of hydrate phases by means of a convergence between a statistical thermodynamics approach implementing

Kihara parameters and a classical approach with a reference state parameters. In a recent publication (Herri and Chassefière, 2012), the Kihara parameters have been optimized to fit equilibrium data at low temperature concerning Martian atmospheric components: carbon dioxide (95.3%), nitrogen (2.7%), Argon (2%) and methane (<50ppb with an average at 15 ppb) (Owen et al., 1977; Mumma et al., 2009), using Handa and Tse (1986) reference state parameters. We observed that the stability of clathrate hydrate is firstly dependent on the partial pressure of carbon dioxide. However, the possible presence of SO_2 in the ancient Mars' atmosphere, a potential promoter for clathrate hydrate formation, could move the stability line for clathrate hydrate formation.

To test the influence of SO_2 we must implement in our models its Kihara parameters, retrieved from experimental data. Up to date, only few equilibrium data have been measured for sulfur dioxide. Above 0°C there are 36 equilibrium data from Van Berkum and Diepen (1979) in the range of temperature [285.2-293.84 K] and the range of pressure [0.253-392.330 MPa], and 2 equilibrium data at (280.2 K, 0.101 MPa) and (273.2 K, 0.0396 MPa) from Von Stackelberg (1949). Below 0°C Tamman and Krige (1925) measured the following experimental points: (261.15 K, 0.01695 MPa), (265.15 K, 0.01997 MPa), (269.15 K, 0.02597 MPa), (270.15 K, 0.02778 MPa), (271.15 K, 0.03051 MPa). Above 0°C, the data can not be easily used to constrain the Kihara parameters because it implies to describe the liquid phase in the presence of salts resulting from SO_2 dissolution (H_2SO_4, HSO_4^-, HSO_4^{2-}) and thus to model the speciation of the reaction as well as the activity coefficient of water. Below 0°C the situation is easier, dealing with ice, simplifying the equations. From a practical point of view, the restricted range of available temperature and pressure measurements hampers the possibility of retrieving only one set of Kihara parameters, but only interdependent sets of values. Our aim is to test within these sets of constrained values the consequence on the composition of (CO_2-SO_2) clathrate hydrate under Martian conditions.

The detailed description of the statistical-thermodynamic model and the strategy used for the retrieval of the SO_2 Kihara parameters required for the modeling are deferred to Appendix A. We, however, stress the importance of this aspect, defining the central parameters on which are based the scientific discussion outcomes in the following sections.

3.2 Extrapolation of experimental data to Martian temperatures

We explored the minimization in the full 3D parameter space (see appendix A) to deduce the minimum SO_2 enrichment during the formation of a mixed SO_2-CO_2 clathrate hydrate in contact with a CO_2 dominated atmosphere. Whatever the minimized set of Kihara parameters for SO_2, and exploring concentration ratios from 0.1 ppm to 1000 ppm of SO_2 in CO_2, the resulting mixed clathrate hydrate formed is always highly enriched in SO_2, by a factor above 60 with respect to gas phase, for all temperatures in the 170-240 K range (Fig.3).

Fig. 3

Falenty et al. (2011) performed experimental kinetics studies of CO_2 clathrate hydrate, monitoring the formation through the neutron diffraction pattern of hexagonal ice in the 185-195 K range. The data were extrapolated at low temperature through a model to compare with the actual polar frosts of Mars, at about 150 K, in order to show that the formation timescale for micron sized clathrates was longer than the typical seasonal variations regularly inducing the declathration. The nucleation rate depends not only on the temperature but on the ice grain sizes when nucleating pure clathrate hydrate from ice aerosol, as the nucleation proceeds in at least two steps: first surface nucleation followed by growth of the hydrate crystal. At 195 K, for a distribution of ice particles of about 1.5 micron of mean equivalent sphere radius, the nucleation proceeds in about one day in the laboratory. Extrapolating at the higher temperatures considered in Fig. 3 for the ancient Martian surface temperature, the nucleation

rate for hydrate formation of similar size ice grains would be higher by a factor of 3 at 200 K to 2 orders of magnitude at 230 K. Precise nucleation timescale with an SO_2-CO_2 clathrate is difficult to extrapolate only based on these experiments, and will depend on the particular mechanism by which the aerosols or surface clathrate kinetic formation proceed (heterogeneous nucleation, diffusion controlled,…), but if we take the high rate of hydrate nuclei growth, it seems reasonable to grow grains as large as 100 microns in hours to days.

4. Modeling of the effects of SO_2 and sulfate aerosols on surface temperature and consequences of CO_2-SO_2 clathrate formation on early Mars climate

For modeling the effects of SO_2 and sulfate aerosols on surface temperature we used the 1-D radiative-convective climate model and the 1-D photochemical model in T10, which allows us to investigate the combined climate effect of CO_2, SO_2, and sulfate aerosols. Most of the model details are described in T10 and will not be repeated here. SO_2 in the early Mars atmosphere could have originated from volcanic outgassing, which is simulated by assuming different surface upward fluxes of SO_2 and H_2S. The ratio between the two species is kept at unity, and previous sensitivity tests (T10) showed that modifying this ratio does not change the results of the photochemical and climate calculations significantly. In this work the relative solar luminosity is set to S/S_0=0.75. The atmospheric pressure is set to the following levels : 1.5, 1, and 0.5 bar, in addition to the level of 3 bar already studied in T10, and Figure 4 shows the relationship between surface temperature and atmospheric SO_2 concentration under different CO_2 pressures. As discussed in T10 the surface temperature increases with enhanced level of atmospheric SO_2 at first because of the greenhouse contribution from SO_2. Nevertheless, as atmospheric SO_2 concentration keeps increasing, photochemistry leads to the formation of sulfate aerosols which can reflect sunlight and cause surface cooling. The

Fig. 4

365 decrease of surface temperature with increasing atmospheric SO_2 is more dramatic under
366 higher CO_2 pressure than under the lower CO_2 pressure because the sulfate aerosols fall
367 slower in a denser atmosphere. It can be seen from Figure 4 that the maximum surface
368 temperatures from combined greenhouse effect of CO_2 and SO_2 in early Martian atmosphere
369 are 235, 235, 230, and 220 K under 3, 1.5, 1.0, and 0.5 bar CO_2 pressure respectively. Thus
370 volcanic outgassing of SO_2 is not a solution to an early warm and wet Mars, consistent with
371 the conclusion in T10.
372
373 For p_{CO2} = 3 bar, the curve is everywhere below the CO_2 clathrate equilibrium temperature.
374 Black triangles in Figure 4 correspond to the SO_2 mixing ratio for which the surface
375 temperature is equal to the CO_2 clathrate equilibrium temperature. The same values are
376 plotted as a function of p_{CO2} in Figure 5. In the four cases (p_{CO2} = 0.5, 1, 1.5 and 3 bar), we Fig. 5
377 have indicated the lava volumes required to give rise to the corresponding SO_2 mixing ratio
378 (Wilson and Head, 2002; Hanna and Phillips, 2006). For a CO_2 pressure larger than 2 bar that
379 may be reached sporadically due to seasonal/orbital effect or also to the CO_2 outgassing from
380 the crust (volcanism and disruption of carbonates), CO_2 clathrates are stable whatever the SO_2
381 mixing ratio in the atmosphere, resulting in the trapping of the fraction of atmospheric CO_2 in
382 excess of 2 bar in the cryosphere under clathrate form. Any atmospheric sulfur released by
383 volcanism is trapped in the cryosphere under the form of CO_2-SO_2 clathrate. Occasionally an
384 SO_2 mixing ratio of ~ 1 ppm may be reached since at this level, sulfur has no significant
385 effect on the mean temperature. For higher values, the surface cooling down will result in
386 CO_2-SO_2 clathration. Note that an ample reservoir of H_2O is available in polar caps (a several
387 10-m thick global equivalent layer in present conditions, probably much more during the
388 Noachian) to feed the formation of clathrates. As soon as an atmospheric H_2O molecule is
389 consumed in clathrate formation, it is replaced by a molecule sublimated from the polar caps,
390 due to the short dynamical time scale of the atmosphere (a few weeks). In terms of reservoirs,
391 the required quantities of H_2O (and CO_2) for all S released by volcanism during the Noachian

to be stored in clathrates is discussed later in this section. H_2S either is converted into SO_2 within the atmosphere in a typical time of a couple of weeks (Wong and Atreya, 2003), or is trapped directly in clathrates.

In the 0.5-2 bar p_{CO2} range, the SO_2 level in the atmosphere following a volcanic eruption can reach typically 10 ppm or so, the excess being trapped in the cryosphere. According to the estimate of the characteristic growth time of a clathrate particle in the atmosphere made in Section 3 (a few hours to days for a 100 µm size particle), trapping occurs rapidly, simultaneously with the radiative cooling of the atmosphere due to sulfate particle formation, which occurs within a few months after SO_2 outgassing. After large volcanic events, the surface temperature is therefore stabilized at the CO_2-SO_2 clathrate equilibrium temperature (~220 K, see Fig. 2) within a few months. Some of the SO_2 trapped in the cryosphere at previous times when p_{CO2}>~2 bar (if it ever occurred) may similarly be released to the atmosphere. Also, the release of a few thousand cubic kilometers of lava may have happened frequently during Tharsis formation (Johnson et al., 2008, and references therein). During this period, the atmosphere could have been rich in SO_2 and sulfate particles (often at equilibrium condition described in Fig.5) and the SO_2-rich cryosphere could have lost part of its SO_2.

For a CO_2 pressure below 0.5 bar, there is no more formation of CO_2-SO_2 clathrates for SO_2 mixing ratio < 200 ppm and all the released sulfur is converted to sulfates. A 200 ppm level of SO_2 in the atmosphere corresponds to the most important eruption supposed to have taken place on Mars, with a lava volume of 50 000 km^3 (Wilson and Head, 2002).

The potential consequences of CO_2-SO_2 clathrate formation on early Mars climate are multiple. Let assume that the CO_2 pressure has been buffered at 2 bar during most of the Noachian. Whereas, during the time when p_{CO2}>~2 bar, there is no SO_2 in the atmosphere and

418 a progressive storing of SO_2 in the cryosphere, the drop of the CO_2 pressure below 2 bar
419 results in the appearance of SO_2 and sulfate aerosols in the atmosphere, due to both episodic
420 volcanism and continuous release of SO_2 previously stored in the cryosphere, with the
421 subsequent acidification and formation of sulfate minerals at the surface. The cryosphere is
422 progressively depleted in SO_2. At this time, if a significant level of the SO_2 mixing ratio is
423 maintained in the atmosphere, including during the periods between volcanic eruptions due to
424 the continuous SO_2 release from the SO_2-rich cryosphere, the surface temperature is stabilized
425 close to the CO_2 clathrate equilibrium temperature of ~220 K (210-230 K in the p_{CO2} range
426 from 1-2 bar). Interestingly, the time when the CO_2 pressure dropped below 2 bar, resulting in
427 sulfate precipitation at the surface, subsequent acidification of the surface and formation of
428 sulfate minerals, could coincide with the age of sulfate minerals observed by OMEGA/ Mars
429 Express (Bibring et al., 2006). If so, the CO_2 pressure had to be of the order of 2 bar at the late
430 Noachian/ Hesperian transition.
431
432 The chronology of clays, sulfates and ferric oxides proposed by Bibring et al. (2006) is shown
433 in Figure 6. We have scaled the CO_2 evolution profile calculated by Chassefière and Leblanc Fig. 6
434 (2011a) by multiplying p_{CO2} by 2.5, in such a way to fit a pressure of ~2 bar at the end of the
435 Noachian, just before sulfate minerals observed by OMEGA were emplaced. The estimated
436 time profile of the crust production rate is also shown (Greeley and Schneid, 1991). The
437 vertical grey band corresponds to the time interval when volcanic activity was significant
438 according to Greeley and Schneid estimates. If the CO_2 pressure dropped below 2 bar at the
439 end of the Noachian, the high volcanic activity during the first half of the Hesperian, when
440 observed sulfate minerals formed, together with the release of SO_2 trapped in the cryosphere
441 during Noachian volcanic events, should have resulted in the precipitation of large amounts of
442 sulfate aerosols, with subsequent acidification of the surface and formation of sulfate minerals.
443 The transformation of the volatile SO_2 from accessible near-surface clathrate reservoir, stored

444 in the Noachian 2-bar regime, to sulfate sediment reservoir is not reversible since there is no
445 efficient sediment recycling on Mars due to plate tectonics. However, Martian impacts may
446 have contributed to recycling. The drop down of surface pressure has permitted the
447 destabilization mechanism to be more and more efficient. The onset of sulfate mineral
448 formation would have been triggered by the drop in CO_2 pressure below 2 bar. The end of
449 sulfate mineral formation would be due to the sharp decrease of volcanic activity at the end of
450 the Hesperian, and the total transformation from CO_2 -SO_2 clathrate to sediment.
451
452 The origin of a possible CO_2 pressure drop at the end of the Noachian is unclear. Non-thermal
453 escape is not expected to have removed more than ~10 mbar during the last 4 Gyr
454 (Chassefière and Leblanc, 2011a). The sink for CO_2 is necessarily within the crust and
455 formation of carbonates in subsurface hydrothermal systems may seem a good candidate
456 (Griffith and Shock, 1995; Chassefière and Leblanc, 2011a). The reason for a stage of intense
457 hydrothermalism at the early Hesperian could be the occurrence of a global scale episode of
458 fissural volcanism between 3.8 and 3.6 Ga (Ody et al., 2012). The olivine-rich magma could
459 have reached the surface through fractures and cracks in the basement rock caused by impacts
460 during the late heavy bombardment (Ody et al., 2012). Such a context, with a highly fractured
461 upper crust filled with both magma and liquid water from the melting cryosphere, may have
462 favored the circulation of CO_2-rich hot waters in the subsurface and the deposition of
463 carbonates in crustal cold water pools (Chassefière and Leblanc, 2011a). This episode could
464 also be responsible for the trapping of large amounts of water in the crust by serpentinization
465 (Chassefière and Leblanc, 2011b). Because in the same time, according to the massive sulfur
466 precipitation scenario, the cryosphere would have lost most of its SO_2, less and less acidic
467 conditions would have prevailed in the subsurface hydrosphere, making more and more
468 efficient the precipitation of carbonates. These hypotheses remain to be confirmed by further
469 studies.

Assuming (i) 2×10^{21} to 5×10^{21} g as the total sulfur degassed in the Noachian by the Tharsis province (Gaillard et al. 2009), (ii) an equilibrium flux of S outgassing and sulfate precipitation in the range from 2×10^{9} to 2×10^{10} molecule $cm^{-2}s^{-1}$ for an atmospheric SO_2 mixing ratio in the range from 1 to 200 ppm (T10), we can estimate that the complete S content from the clathrate reservoir is released in a time range from 40 to 1000 Myrs. The cryosphere in the Noachian 2-bar regime has to be quite rich in SO_2. Assuming for example a SO_2/CO_2 ratio in the clathrate of 20%, the required water GEL thickness is in the range from 250 to 630 m, for a CO_2 global equivalent pressure in the range from 3 to 7.5 bar. A twice lower ratio of 10% results in twice higher H_2O and CO_2 inventories (500-1300 m/ 6-15 bar). A twice larger ratio of 40% results in twice lower H_2O and CO_2 inventories (125-315 m/ 1.5-3.7 bar). These orders of magnitude estimates are reasonable for the global inventory of Martian volatiles, as described in Section 1, implying a SO_2/CO_2 ratio in the clathrates of several tens percents. If the sulfate is deposited in form of anhydrite (Gaillard et al. 2009) at 136 $g.mol^{-1}$, it will precipitate in a 20 to 50 m global layer.

Two majors geomorphological units are compatible with our scenario:

1) The presence of a thick Mars-wide sedimentary formation of sulfate, including in very uncommon places at high topography, such the Interior Layer Deposit (ILD) at the top of Valles Marineris. Eolian deposition was proposed from geomorphological arguments (Michalski et al., 2011). For ILD in Valles Marineris, the formation as thick as 5 km (Nedell et al., 1987) must be done in 400 Myrs, after the tectonic opening at 3.9 Ga and the formation of the floor 3.5 Ga (Quantin et al., 2004). In our scenario, 20 m to 50 m GEL sulfur particle could have precipitated directly from atmosphere in 40 to 1000 Myrs, in agreement with the observation. The sedimentary formation of sulfate seems to be at very large scale (Bibring et

al., 2006) since it has been detected in different places on Mars such as Valles Marineris (Bibring et al., 2007, Le Deit et al, 2008), Meridiani Planum (Squyres et al., 2004), Aram Chaos (Massé et al., 2008) and Syrtis Major (Ehlmann et al., 2012).

2) The chaotic terrains, at equatorial region, could have been formed by disruption of the CO_2 clathrate in the past at the late Hesperian/Amazonian period. This interpretation is compatible with our scenario since the formation of clathrate must have been global during the Noachian, it should also affect equatorial region. The reason for such a disruption has been debated, including climatic change (Clifford and Parker, 2001), internal heat flux (Clifford and Parker, 2001), fracture propagation (Rodriguez et al., 2006), and seismic activity (Nummedal and Prior, 1981; Tanaka, 1999). We propose here that the disruption may be due to the pressure decrease below 2 bar. In our scenario, a GEL of CO_2-SO_2 clathrate ranging from 290 m to 720 m depth has been destabilized. Scaling this volume to the province of the chaos (1/10 surface of Mars)is compatible with the typical height loss in chaos ~3000 m. A schematic representation of the evolution of early Mars' under the effect of CO_2-SO_2 clathrate formation and destabilization is shown in Figure 7. Fig.7

As previously stated, the surface temperature of ~230 K proposed to have prevailed during the Noachian is a global average value due to the use of a 1-D model. In the real Martian surface, there are places where the temperature is higher than 230 K, and clathrates don't form, for instance near the equator at low obliquity. They form only in the locations where the temperature reach 230 K, for instance at the pole at low obliquity. Due to the large variations of the obliquity of Mars on typical time periods of 10^5-10^6 yr (Laskar et al., 2002; Levrard et al., 2004), the colder regions of the planet regularly become warmer, and vice versa. We don't know if variations of orbital parameters similar to those calculated for the last ten million years occurred on early Mars. This is still unknown, especially under the scenario of giant

planet migration (Gomes et al., 2005; Morbidelli et al., 2007). Some chaotic variations of obliquity may have occurred at the Noachian (before giant planet migration) in specific dynamical conditions, but in other conditions obliquity may have remained stable (Brasser and Walsh, 2011). Making the hypothesis that early Mars obliquity changed in a similar fashion as it does today, a coming and going of ice deposits, including CO_2-SO_2 clathrates, between high latitude (at low obliquity) and low latitude (at high obliquity) regions through alternate sequences of sublimation and condensation should have occurred. On the recent Mars (last 10 Myr), the typical time scale for ice migration during a transition of the mean obliquity, like that which occurred 4 Myr ago, is ~1 Myr (Levrard et al., 2007). On ancient Mars, where water was more abundant and the CO_2 pressure higher, this time should have been larger. Assuming that the residence time of SO_2 in the atmosphere with respect to clathrate formation on the cold trap is 1 yr (see below), and that the equivalent of 1 bar of SO_2 is transferred in 1 Myr, the average SO_2 mixing ratio in a 2-bar atmosphere during an obliquity transition is 0.5 ppm. For an ice migration time of 10 Myr, and an amount of transferred SO_2 of 0.2 bar, the average SO_2 mixing ratio during obliquity transition is 10^{-2} ppm. These values are small, with no expected effect on climate. An important question is to know if, during its transfer through the atmosphere, SO_2 is preserved from forming aerosols and being removed from the atmosphere-cryosphere system. The residence time of SO_2 in the atmosphere, before being removed by aerosol deposition, is 10^2-10^3 yr (Johnson et al., 2009, T10). The global mixing time of Mars atmosphere is ≈0.5 yr (Krasnopolsky, 2005), of the same order as the Earth troposphere mixing time (≈1 yr). The lifetime of a SO_2 molecule with respect to trapping in clathrates is therefore 2 to 3 orders of magnitude smaller than the time of SO_2 removal by aerosol deposition. SO_2 is therefore expected to survive ice migrations, making possible the preservation of a SO_2-rich cryosphere during the whole Noachian.

547 It must be emphasized that the threshold pressure value of 2 bar is obtained by using the 1-D
548 model. The mean annual surface temperature is not uniform, decreasing from the equator to
549 the poles. On Mars today, regions above 45° latitude in both hemispheres have an annual
550 surface temperature lower by more than 10 K than the global average temperature (see e.g.
551 Mellon et al., 2003). As shown on Figure 2, the difference between the mean global
552 temperature and the CO_2 clathrate formation temperature is smaller than ≈10 K in the range
553 0.5-2 bar. By analogy with present Mars, it results that even with a CO_2 pressure of only 0.5
554 bar, regions above 45° latitude could have been below the clathrate formation temperature in
555 annual average. If so, it may be thought that the cold trap formed by middle and high latitude
556 regions may have been efficient enough to remove most of the SO_2 released to the atmosphere
557 (including in equatorial regions) by volcanism. More accurate 2-D or 3-D models are required
558 to precisely define the value of the pressure threshold, which could be smaller than 2 bar and
559 even possibly 1 bar. Such a lower threshold value would be in better agreement with a strong
560 carbon hydrodynamic escape ruling out a dense Martian atmosphere until the late Noachian
561 (Tian et al., 2009), and the recent estimate of <1 bar obtained from the constraint provided by
562 the $^{40}Ar/^{36}Ar$ ratios of trapped gases within Martian meteorite ALH 84001 (Cassata et al.,
563 2012).
564

565 ## 5. Influence of the presence of SO_2 on the trapping of argon, krypton and
566 ## xenon in clathrates
567

568 Mousis et al. (2012) found recently that it was possible to account for the two orders of
569 magnitude drop existing between the measured atmospheric abundances of non-radiogenic
570 argon, krypton and xenon in Earth versus Mars (see Pepin, 1991) by invoking the trapping of
571 these noble gases in clathrate deposits incorporated into the current Martian cryosphere. In
572 their scenario, these authors estimated that masses of xenon, krypton and argon equivalent to

573 those found on Earth could be incorporated into clathrates if one assumes the simultaneous
574 trapping of at least 2.3 bar of CO_2. This value is quite close to the maximum value of 2 bar
575 imposed by the CO_2 clathrate saturation law, as previously explained, and is therefore
576 compatible with constraints derived from the present work. Mousis et al. (2012) also
577 considered the presence of atmospheric SO_2 on the clathrate composition. In order to quantify
578 the influence of this species on the noble gas trapping in CO_2-dominated clathrate, they used
579 approximate combination rules allowing them to retrieve a set of interaction potential
580 parameters for SO_2-H_2O interactions. They then deduced that this species was a poor clathrate
581 former in the presence of a CO_2-dominated gas and concluded that it has zero influence on the
582 trapping efficiencies of other minor species, including noble gases.
583
584 The set of potential parameters determined for SO_2-H_2O interactions in the present work
585 supersedes the exploratory one used by Mousis et al. (2012) and suggests that the mole
586 fraction of SO_2 can be strongly enriched in CO_2-dominated clathrate compared to that existing
587 in the gas phase. This implies that the question of the influence of this species on the noble
588 gas trapping in CO_2-dominated clathrate remains open. Here we use a gas phase composition
589 similar to the one defined by Mousis et al. (2012), in which the mole fraction of SO_2 is varied
590 between 10^{-3}, 1 and 10^3 ppm, in order to investigate the influence of SO_2 on the trapping of
591 other minor species. Abundances of CO_2, N_2, O_2, CO, Ar, Kr and Xe derive from Moroz
592 (1998). In each of the three cases, the abundance of CO_2 is adjusted to allow the
593 normalization to 1 of the sum of the mole fractions.
594
595 A set of SO_2-H_2O interaction parameters, which is representative of the range of solutions
596 determined in Section 2 and Appendix A, has been selected (a = 0.75 Å, ε/K = 258.91 K and
597 σ = 2.7 Å). These parameters correspond to a mean enrichment factor of 100 of the SO_2 mole
598 fraction in clathrate compared to the atmospheric one at a surface pressure of 1 bar,

irrespective of the considered SO_2 abundance (10^{-3}, 1 and 10^3 ppm). Figure 8 represents the clathrate composition computed in the three cases of the SO_2 abundance for atmospheric pressures up to 3 bar, allowing us to encompass all the plausible values discussed in the literature. At each pressure considered, the temperature used in our computations is the equilibrium temperature of CO_2-dominated clathrate. The figure shows that the mole fractions of minor species are not altered when considering SO_2 atmospheric abundances ranging from 10^{-3} to 1 ppm. At a SO_2 atmospheric abundance of 10^3 ppm, the trapping efficiencies of Ar and Kr are decreased by a factor of 10 and that of Xe is almost unchanged. Fig. 8

Our calculations imply that the conclusions of Mousis et al. (2012) remain valid if one assumes that the SO_2 atmospheric abundance ranges between 10^{-3} and 1 ppm. However, for higher mixing ratios such as those estimated in the Noachian (see Sec. 4), the efficient clathration of SO_2 implies the trapping of up to several dozens of bar of atmospheric CO_2 if one wants to account for the losses or Ar and Kr via their clathration in the cryosphere. Because these values are implausible, it seems that the scenario proposing that the noble gas deficiency of the Martian atmosphere is due to their efficient sequestration in clathrates present in the cryosphere is not consistent with the one proposed here for SO_2.

6. Discussion

We suggested in the present study that the formation of CO_2-SO_2 clathrates at Noachian and Hesperian times could have played an important role in controlling and stabilizing the level of volcanic sulfur in the atmosphere, as well as the level of atmospheric CO_2 for earliest times. If the CO_2 pressure exceeded a threshold of p_0 = 2 bar (possibly less : 0.5-1 bar, which remains to be confirmed from more sophisticated 3D models) due to an efficient Noachian volcanism, the CO_2 in excess of p_0 (assumed to be ~2 bar for the discussion) could have been stored in

625 the cryosphere under the form of CO_2 clathrates. Indeed, due to the increasing albedo of the
626 atmosphere through Rayleigh scattering for increasing CO_2 pressure above 1 bar, the surface
627 temperature induced by a p>~2 bar CO_2 atmosphere is smaller than the equilibrium
628 temperature of clathrates, resulting in a saturation of CO_2 and its condensation under the form
629 of clathrates. Such a clathrate buffer would have maintained the CO_2 pressure close to ~2 bar,
630 and the surface temperature close to 230 K, resulting in a cold Mars at the Noachian. The
631 cryosphere would have trapped all the sulfur released by volcanism under the form of sulfur-
632 rich (enriched by a factor ~100-500 with respect to the gas phase) CO_2-SO_2 clathrates.
633
634 Because the thermal conductivity of clathrates is low, smaller than that of water ice on the
635 order of 5 to 6 times (Mellon, 1996), the formation of clathrate deposits should result in a
636 higher thermal gradient, with an accumulation of heat beneath the clathrate layer. It has been
637 suggested that, on present Mars, no more than a global equivalent atmospheric pressure of
638 112 mbar of CO_2, in a 4-km thick polar deposit, may be contained in the polar caps. For a
639 larger amount of deposited CO_2, the warming at the base of the clathrate layer results in the
640 liquefaction of CO_2, essentially precluding the stability of the system. On early Mars, the
641 deposition of large amounts of CO_2 clathrates, assuming an atmospheric content larger than 2
642 bar, could have led to this kind of instability. But if clathrates were deposited on an extended
643 fraction of the surface, much larger than the present caps, the maximum admissible value of
644 the global equivalent atmospheric pressure of CO_2 trapped in clathrates could be much larger
645 than 112 mbar. This phenomenon should have to be taken into account in any detailed
646 modeling of massive clathrate deposition in the Noachian cryosphere.
647
648 For a surface pressure smaller than 2 bar and progressively decreasing, atmospheric sulfur is
649 no longer trapped in clathrates, and an increasing fraction of the atmospheric SO_2, up to 10
650 ppm at p_{CO2}=1.5 bar, and 30 ppm at p_{CO2}=1 bar, can remain in the atmosphere. If the amount

651 of atmospheric SO_2 exceeds these thresholds, the cooling effect of sulfate aerosols results in a
652 decrease of surface temperature below the clathrate equilibrium temperature and the
653 condensation of the SO_2 in excess in CO_2-SO_2 clathrates. During this period, significant
654 amount of SO_2 (and H_2S rapidly converted in SO_2 by atmospheric photochemistry) was
655 converted into sulfate aerosols, which further settled down to the surface and possibly led to
656 the formation of sulfate minerals. This sulfur may have been released, not only by volcanoes
657 but also (and more continuously) by the SO_2-rich cryosphere formed when p_{CO2}>~2 bar.
658 Through this mechanism, the cryosphere may have lost at this stage some of the volcanic SO_2
659 stored at earlier times, released back to the atmosphere. In this time range (2 to 1 bar p_{CO2}
660 range), the surface temperature has been buffered, during and after episodes of sulfur release,
661 at a temperature from 230 K (p_{CO2}=2 bar) to 210 K (p_{CO2}=1 bar). For p_{CO2}<1 bar, all the
662 released SO_2 remains in the atmosphere, with no more trapping in clathrates.
663
664 We proposed the hypothesis that the formation of sulfate minerals, which have been observed
665 from orbit and are formed during the Hesperian (Bibring et al., 2006), could have been
666 triggered by a fall of early Mars atmosphere pressure below 2 bar and that this change
667 occurred close to the late Noachian/Hesperian transition. This hypothesis requires that the
668 total amount of CO_2 in both the atmosphere and the cryosphere during the Noachian has been
669 greater than the content of a 2 bar atmosphere as a result of substantial volcanic outgassing
670 and/or rapid carbonate formation, which might have been efficient enough to keep some CO_2
671 on early Mars despite rapid carbon escape. This constraint could be alleviated if further 3D-
672 modeling shows that a pressure threshold value of 0.5-1 bar is sufficient to keep most of the
673 released SO_2 trapped under clathrate form in the Noachian cryosphere. According to our
674 hypothesis, Mars' cryosphere would have stored under the form of CO_2-SO_2 clathrates a
675 significant amount of the sulfur outgassed during the whole Noachian (from the magma ocean
676 crystallization to the 2-bar transition). At the transition between Noachian and Hesperian, this

reservoir would have been released back into the atmosphere through clathrate disruption that may be at the origin of the chaotic terrains. Then sulfur has precipitated in the form of aerosols, creating a large-scale sulfate deposit, in agreement with several in-situ and orbital observations. Today, the sulfate layer is not present everywhere but observed in some places such Valles Marineris (Bibring et al., 2007, Le Deit et al, 2008), Meridiani Planum (Squyres et al., 2004), Aram Chaos (Massé et al., 2008) and Syrtis Major (Ehlmann et al., 2012). First, the net aerosols precipitation flux in the ancient Mars should be controlled by local winds and topography in an analogous manner than snow precipitation (Forget et al., 2006). Second, the erosion may have removed significant part of the initial layer, especially because sulfate is highly transportable in soluble phase, such kieserite.

According to our scenario, the formation of carbonates should have been inhibited (at least in the superficial cryosphere) during most of the Noachian, although probably not at earliest times when the cryosphere was still SO_2-free, due to the acidification of water resulting from the local melting of the SO_2-rich cryosphere. Such fluid can precipitate sulfate phase locally in the subsurface but the cryosphere may be SO_2-rich enough (it can potentially store the complete SO_2 degassed from volcanism, see Sec. 4) implying unlikely conditions for carbonates precipitation. As previously mentioned it may be thought that during the massive release of SO_2 to the atmosphere after the end of the 2-bar stage at the Noachian-Hesperian transition, and the subsequent sequestration of sulfur in sediments, a less acidic cryosphere allowed the formation of carbonates, relatively deep in the subsurface due to cold and acidic surface conditions. Because the trapping of CO_2 in carbonates results in a decrease of the atmospheric pressure, and therefore a release of SO_2 to the atmosphere and its further sequestration in sediments, a positive feedback could have occurred. The removal of CO_2 in carbonates would have allowed SO_2 to be released and trapped in sulfate sediments, decreasing the acidity of the cryosphere and allowing more carbonates to be formed. Such a

703 runaway process could be one of the reasons for the sharp decrease of atmospheric CO_2
704 during the Hesperian, simultaneously with the formation of large sediment deposits, but
705 remains a hypothesis to be further explored.
706
707 According to our scenario in the pre-Noachian and Noachian periods, the massive presence of
708 sulfur in the cryosphere/atmosphere has kept low global temperature (near 230 K), in
709 agreement with the results of clay minerals observations (Ehlmann et al., 2011). Under such
710 conditions, clays may have been formed by alteration of the crust in the locally warmer
711 region, where no SO_2-CO_2 clathrate can condense (equator during low obliquity). The low
712 atmospheric SO_2 gas content may lead to acidic pH preventing carbonate from precipitating
713 but permitting clay formation near the surface. More detailed modeling are required to discuss
714 these implications.
715
716 Interestingly, the massive presence of sulfur in the pre-Noachian and Noachian cryosphere
717 could have favored the occurrence of warm episodes, with liquid water at the surface and a
718 global hydrological cycle. Such a warm episode, or series of warm episodes, with a typical
719 duration of 10^5-10^7 years, could have allowed the formation of valley networks observed in
720 the southern hemisphere (Hoke et al., 2011), and formed close to the late Noachian/
721 Hesperian transition. Similar episodes seem to be required at the middle Noachian to explain
722 the high degree of degradation of ancient craters (N. Mangold, personal communication,
723 2012). It has been suggested that SO_2, in addition to CO_2, could have played a major role in
724 maintaining water in a liquid state at the surface of Mars for significant periods of time, with
725 an ocean and a global hydrological cycle, and that such an episode could have been controlled
726 by a well-developed SO_2 cycle (Halevy et al., 2007). The major objection in our scenario is
727 that, starting from a cold state, any release of SO_2 to the atmosphere is followed by the
728 formation of sulfate aerosols and a subsequent cooling of the atmosphere (T10). But any

729 catastrophic event such as a giant asteroid impact or a massive volcanic SO_2 release or a
730 large-scale destabilization of methane clathrate from a highly magmatically active subsurface,
731 might have been able to melt the superficial cryosphere and release huge amounts of SO_2 and
732 H_2O (and possibly CO_2) into the atmosphere. Provided such a catastrophic event was able to
733 trigger a global hydrological cycle, even for a short time of a few years or hundred years, the
734 SO_2 (and CO_2) released at the same time from the melting cryosphere could have taken the
735 relay and driven a somewhat longer period of warm and wet Mars, according to Halevy et al.
736 scenario. Episodes of huge methane release from clathrates present on oceanic floors occurred
737 during the history of Earth. At the Paleocene-Eocene transition, 55.5 Myr ago, massive
738 dissociation of oceanic methane hydrate led to a warming of 5-6 °C during ~1000 yr (see e.g.
739 Higgins and Schrag, 2006). The injection of CH_4 into early Mars atmosphere with a mixing
740 ratio of a few percents, that is partial pressure of a few tens millibar, may have possibly raised
741 the surface temperature above 0°C (Kasting, 1997), but further calculations by Tian
742 (unpublished) don't confirm that CH_4, even at several percent level, is able to bring surface
743 temperature close to the freezing point of water. Understanding if massive methane injections
744 in the atmosphere of Mars, and/or giant impacts, have been able to initiate a SO_2 cycle-driven
745 episode of warm and wet Mars (Halevy et al., 2007), breaking the background cold Noachian
746 climate, is of prime interest to progress in our understanding of early Mars climate.
747
748 Whatever the precise triggering mechanisms of such possible warm episodes favored by the
749 release of massive amounts of SO_2 together with CO_2 to the atmosphere may have been, our
750 hypothesis may potentially explain the occurrence of outflow channels, valley networks and
751 the degradation of impact craters. In Sec. 4, we suggested that the destabilization of clathrates
752 when p_{CO2} dropped below 2 bar could be at the origin of chaotic terrains, and it may therefore
753 as well explain the formation of outflow channels, provided sufficient amounts of water were
754 present in the subsurface. Valley networks, formed at the late Noachian and which ended

755 relatively sharply at the beginning of the Hesperian (Fasset and Head, 2011), could be the
756 result of warm episodes occurring when the CO_2 pressure was still close to 2 bar, and the
757 temperature relatively “high” (230 K). Such episodes could explain the formation of some
758 sulfate deposits during the Noachian. The postulated drop in pressure at the
759 Noachian/Hesperian transition resulted in a general cooling of the planet from 230 K to 220 K
760 (for p_{CO2}=1 bar), then 210 K (for p_{CO2}=0.5 bar) (see Fig. 2). Provided this drop was sharp
761 enough, the cooling of the planet by ≈20 K during the Hesperian could have rapidly inhibited
762 warm episodes possibly at the origin of valley networks. A recent study shows that the
763 degradation of impact craters experienced a sharp transition at 3.7 Ga (Mangold et al., 2012).
764 This transition between a period of substantial erosion due to a significant global fluvial
765 activity (late Noachian) and a period of more regional and sporadic warming episodes
766 (Hesperian) may be the result of the suggested drop in pressure, resulting in both a general
767 cooling of the planet and episodes of massive SO_2-CO_2 release. The necessarily sporadic
768 nature of clathrate destabilization during the Hesperian could be at the origin of the
769 degradation of Hesperian craters, showing no relationship between age and degradation state
770 (Mangold et al., 2012). In order to confirm these views, it will be necessary to build reliable
771 scenarios of such warming episodes, possibly triggered by specific events (impacts, massive
772 methane release, obliquity variations…) and favored by massive SO_2 release together with
773 CO_2. If these events are intense enough, liquid water precipitation (rain) may incorporate
774 atmospheric SO_2 so that the SO_2 aerosol deposition time could be shorter than in our arid
775 model (SO_2 aerosols precipitation), implying a reduced cooling effect of aerosols, not
776 sufficient to counteract the warming effect of SO_2 and other greenhouse gases. These extreme
777 events provide also SO_2 precipitation before the Noachian-Hesperian boundary that could
778 explain observed geological units. Also, clays may have been formed during such favorable
779 climatic excursions (see e.g. Fan et al., 2008 ; Murchie et al., 2009 ; Wray et al., 2011).
780

781 Our results are based on extrapolations to low temperatures of the results obtained in Earth's
782 laboratory conditions. In order to progress in our understanding of the role of the sulfur cycle
783 in the early evolution of Mars, experimental measurements devoted to the measurements of
784 CO_2-SO_2 clathrates thermodynamical and kinetic properties in Martian conditions would be
785 necessary. Future space missions to Mars could also bring new results. Search for SO_2 plumes
786 associated with outgassing from surviving buried cryospheric SO_2 clathrate-rich reservoirs by
787 the Exomars TGO mission in 2016, and mapping of SO_2 (if detected), could help in
788 characterizing a possible residual activity of sulfur in the Martian crust. SO_2 has never been
789 detected in the Martian atmosphere, with a measured upper limit at 2 σ of 1 ppb
790 (Krasnopolsy, 2005). Nevertheless, if some SO_2 has been trapped at depth in long life time
791 clathrate layers, an episodic release due to tectonic or subsurface thermal events triggering the
792 destabilization of clathrates cannot be ruled out. The dielectric constants of clathrates are too
793 close to that of water ice to allow to them to be easily distinguished at radar wavelengths
794 (Mousis et al., 2012), which makes subsurface clathrate layers hardly detectable from orbit.
795 Buried reservoirs of SO_2 and H_2S clathrate-hydrates could be searched for through drilling
796 from future landers on Mars. If some sulfur clathrate deposits survived close to some
797 volcanoes, a concentric structure might be observed, like e.g. around the Hakon Mosby mud
798 volcano in Marmara Sea where concentric layers of gas hydrates are observed, with a
799 maximum concentration of clathrates in the sediment of 10-20% at about five hundred meters
800 of the volcano (Fig. II.17 in Bourry, 2008). In a similar way, although in quite different
801 conditions (subaerial volcanism, larger space and time scales), concentric deposits of CO_2-
802 SO_2-H_2S clathrates could have been formed on Mars around volcanoes, with concentrations
803 and composition expected to depend on the distance to the outgassing plume. The possibility
804 for such deposits to have survived a long time is of course highly speculative, and we don't
805 know at which depth they could have been preserved.
806

807 Acknowlegments : E. Chassefière, E. Dartois, A. Lakhlifi and F. Schmidt thank the
808 interdisciplinary EPOV program of CNRS. O. Mousis acknowledges support from CNES. We
809 feel indebted to the referees, M. Mischna and A. Fairén, for their constructive comments that
810 allowed to significantly improve the quality of this paper. We thank L. Daumas for the
811 drawing of figure 7.
812
813 **References :**
814
815 Adisasmito, S., Frank, R.K., Sloan, E.D., 1991, J. Chem. Eng. Data, 36, 68-71.
816 Baldridge, A. M., Hook, S. J., Crowley, J. K., Marion, G. M., Kargel, J. S., Michalski, J. L.,
817 Thomson, B. J., de SouzaFilho, C. R., Bridges, N. T., Brown, A. J., 2009.
818 Contemporaneous deposition of phyllosilicates and sulfates: Using Australian acidic saline
819 lake deposits to describe geochemical variability on Mars, Geophys. Res. Lett. 36, L19201,
820 doi:10.1029/2009GL040069.
821 Bibring, J.-P., Langevin, Y., Mustard, J. F., Poulet, F., Arvidson, R., Gendrin A., Gondet, B.,
822 Mangold, N., Pinet, P., Forget, F., 2006. Global Mineralogical and Aqueous Mars History
823 Derived from OMEGA/Mars Express Data, Science 312, 5772, 400-404.
824 Bibring, J.-P., Arvidson, R. E., Gendrin, A., Gondet, B., Langevin, Y., Le Mouelic, S.,
825 Mangold, N., Morris, R. V., Mustard, J. F., Poulet, F., Quantin, C., Sotin, C., 2007,
826 Coupled Ferric Oxides and Sulfates on the Martian Surface, Science 317, 1206-1210.
827 Bourry, C., 2008. Caractérisation physique et géochimique d'hydrates de gaz
828 d'environnements géologiques différents, PhD thesis, University of Brest, France.
829 Brasser, R., Walsh, K.J., 2011. Stability analysis of the Martian obliquity during the Noachian
830 era, Icarus 213, 423–427.

831 Cassata, W.S., Shuster, D.L., Renne, P.R., Weiss, B.P., 2012.Trapped Ar isotopes in
832 meteorite ALH 84001 indicate Mars did not have a thickancientatmosphere, Icarus 221,
833 461–465.
834 Chassefière, E., Leblanc, F., 2011a. Methane release and the carbon cycle on Mars. Planet.
835 Space Sci. 59, 207-217.
836 Chassefière, E., Leblanc, F., 2011b. Constraining methane release due to serpentinization by
837 the D/H ratio on Mars, Earth Planet. Sci. Lett. 310, 262–271.
838 Christensen, P., 2006. Water at the Poles and in Permafrost Regions of Mars,
839 Elements 2, 151-155.
840 Clifford, S. M., Parker, T. J., 2001, The Evolution of the Martian Hydrosphere: Implications
841 for the Fate of a Primordial Ocean and the Current State of the Northern Plains, Icarus 154,
842 40–79.
843 Clifford, S.M., Lasue, J., Heggy, E., Boisson, J., McGovern, P., Max, M.D., 2010. Depth of
844 the Martian cryosphere: Revised estimates and implications for the existence and detection
845 of subpermafrost groundwater, J. Geophys. Res. 115, E07001, doi:10.1029/2009JE003462.
846 Colaprete, A., Toon, O. B., 2003. Carbon dioxide clouds in an early dense Martian
847 atmosphere. J. Geophys. Res. 108, 5025, doi:10.1029/2002JE001967.
848 Craddock, R. A., Greeley, R., 2009. Minimum estimates of the amount and timing of gases
849 released into the martian atmosphere from volcanic eruptions. Icarus. 204, 512-526.
850 Danesh, A., 1998, Phase Behaviour of Petroleum reservoirs Fluids, Elsevier Science BV,
851 ISBN 0444821861.
852 Ehlmann, B.L., Mustard, J.F., Murchie, S.L., Bibring, J.-P., Meunier, A., Fraeman, A.A.,
853 Langevin, Y., 2011. Subsurface water and clay mineral formation during the early history
854 of Mars, Nature 479, 53, doi:10.1038/nature10582.
855 Ehlmann, B. L., Mustard, J. F., 2012, An in-situ record of major environmental transitions on
856 early Mars at Northeast Syrtis Major, Geophys. Res. Lett., 39, L11202.

857 Fairén, A. G., et al., 2004. Inhibition of carbonate synthesis in acidic oceans on early Mars.
858 Nature. 431, 423-426.
859 Falabella, B.J., Vanpee, M., 1974. Experimental Determination of Gas Hydrate Equilibrium
860 below the Ice Point. Ind. Eng. Chem. Fundam.13, 228-231.
861 Falenty A., Genov G., Hansen Th. C., Kuhs W. F., Salamatin A. N., Falenty, 2011, Kinetics
862 of CO_2 Hydrate Formation from Water Frost at Low Temperatures: Experimental Results
863 and Theoretical Model**.** J. Phys. Chem. C 115, 4022–4032.
864 Fan, C., Schulze-Makuch, D., Fairén, A.G., Wolff, J.A., 2008. A new hypothesis for the
865 origin and redistribution of sulfates in the equatorial region of western Mars, Geophys.
866 Res. Lett. 35, L06201, doi:10.1029/2007GL033079.
867 Fasset, C. I., Head, J.W., 2011. Sequence and timing of conditions on early Mars, Icarus 211,
868 1204–1214.
869 Forget, F., Pierrehumbert, R. T., 1997. Warming Early Mars with Carbon Dioxide Clouds
870 That Scatter Infrared Radiation. Science. 278, 1273-1276.
871 Forget, F., Haberle, R. M., Montmessin, F., Levrard, B. & Head, J. W., 2006, Formation of
872 Glaciers on Mars by Atmospheric Precipitation at High Obliquity, Science, 311, 368-371
873 Gaillard, F., Scaillet B., 2009. The sulfur content of volcanic gases on Mars. Earth Planet. Sci.
874 Lett., 279, 1-2, 34-43.
875 Gaillard, F., Michalski, J., Berger, G., McLennan, S., Scaillet, B., 2012. Geochemical
876 reservoirs and timing of sulphur cycling on Mars, Space Sci. Rev., in press, doi
877 10.1007/s11214-012-9947-4.
878 Gomes, R., Levison, H., Tsiganis, K., Morbidelli, A., 2005, Origin of the cataclysmic Late
879 Heavy Bombardment period of the terrestrial planets, Nature 435, 466-469.
880 Griffith, L. L., Shock, E. L., 1995. A Geochemical Model for the Formation of Hydrothermal
881 Carbonates on Mars. Nature. 377, 406-408.

882 Greeley, R., Schneid, B.D., 1991. Magma generation on Mars - Amounts, rates, and
883 comparisons with earth, moon, and Venus, Science 254, 1991, 996-998.
884 Grott, M., et al., 2011. Volcanic outgassing of CO_2 and H_2O on Mars. Earth and Planetary
885 Science Letters. 308, 391-400.
886 Halevy, I., Zuber, M. T., Schrag, D. P., 2007. A Sulfur Dioxide Climate Feedback on Early
887 Mars, Science 318, 5858, 1903-1907.
888 Handa, Y.P. , Tse, J.S., 1986, Thermodynamic properties of empty lattices of structure I and
889 structure II clathrate hydrates, J. Phys. Chem. 23, 5917-5921.
890 Hanna, J. C., Phillips, R.J., 2006, Tectonic pressurization of aquifers inthe formation of
891 Mangala and Athabasca valles, Mars, J. Geophys. Res. 111, E03003,
892 doi:10.1029/2005JE002546.
893 Head, J. W., Pratt, S., 2001. Extensive Hesperian-aged south polar ice sheet on Mars:
894 Evidence for massive melting and retreat, and lateral flow and ponding of meltwater, J.
895 Geophys. Res. 106, E6, 12275-12300.
896 Head, J. W., Marchant, D. R., 2009. Inventory of Ice-related Deposits on Mars: Evidence for
897 Burial and Long-Term Sequestration of Ice in Non-Polar Regions and Implications for the
898 Water Budget and Climate Evolution, 40th Lunar and Planetary Science Conference,
899 (Lunar and Planetary Science XL), March 23-27, 2009 in The Woodlands, Texas, id.1356.
900 Herri, J.-M., Bouchemoua, A., Kwaterski, M., Fezoua, A., Ouabbas, Y., Cameirao, A., 2011.
901 Gas Hydrate Equilibria from CO_2-N_2 and CO_2-CH_4 gas mixtures – Experimental studies
902 and Thermodynamic Modelling. Fluid Phase Equilibria 301, 171-190.
903 Herri, J.M., Chassefière, E., 2012, Carbon dioxide, argon, nitrogen and methane clathrate
904 hydrates: thermodynamic modelling, investigation of their stability in Martian atmospheric
905 conditions and variability of methane trapping, Planet. Space Sci., in press, doi
906 10.1016/j.pss.2012.07.028.
907 Higgins, J.A., Schrag, D.P., 2006. Beyond methane: Towards a theory for the Paleocene–

EoceneThermal Maximum, Earth Planet. Sci. Lett. 245, 523-537.

Hoke, M. R. T., Hynek, B.M., Tucker, G.E., 2011, Formation timescales of large Martian valley networks, Earth Planet. Sci. Lett. 312, 1-12.

Johnson, S. S., Mischna, M. A., Grove, T. L., Zuber, M. T., 2008. Sulfur-induced greenhouse warming on early Mars, J. Geophys. Res. 113, E8, CiteID E08005.

Johnson, S.S., Pavlov, A.A., Mischna, M.A., 2009. Fate of SO_2 in the ancient Martian atmosphere: Implications for transient greenhouse warming, J. Geophys. Res. 114, E11011, doi:10.1029/2008JE003313.

Kasting, J.F., 1997. Warming early Earth and Mars, Science 276, 1213-1215.

King, P.P., McLennan, S.M., 2010. Sulfur on Mars, Elements 6, 107-112.

Krasnopolsky, V.A., 2005. A sensitive search for SO_2 in the martian atmosphere: Implications for seepage and origin of methane, Icarus 178, 487–492.

Laskar, J., Levrard, B., Mustard, J. F. 2002. Orbital forcing of the martian polar layered deposits. Nature 419, 375–377.

Le Deit, L., Le Mouélic, S., Bourgeois, O., Combe, J.-P., Mège, D., Sotin, C., Gendrin, A., Hauber, E., Mangold, N., Bibring, J.-P., 2008, Ferric oxides in East Candor Chasma, Valles Marineris (Mars) inferred from analysis of OMEGA/Mars Express data: Identification and geological interpretation», J. Geophys. Res.113, Issue E7, CiteID E07001.

Levrard, B., Forget, F., Montmessin, F., Laskar, J., 2004. Recent ice-rich deposits formed at High latitude on Mars by sublimation of unstable equatorial ice duringlow obliquity, Nature431, Issue 7012, 1072-1075.

Mckoy, V., Sinagoglu, O. J., 1963. Theory of dissociation pressures of some gas hydrates. J Chem. Phys. 38, 2946-2956.

Mangold, N., Adeli, S., Conway, S., Ansan, V., Langlais, B. 2012. A chronology of early Mars climatic evolution from impact crater degradation, J. Geophys. Res. 117, E04003,

934 doi:10.1029/2011JE004005.
935 Massé, M., Le Mouélic, S., Bourgeois, O., Combe, J.-P., Le Deit, L., Sotin, C., Bibring, J.-P.,
936 Gondet, B., Langevin, Y., 2008, Mineralogical composition, structure, morphology, and
937 geological history of Aram Chaos crater fill on Mars derived from OMEGA Mars Express
938 data, J. Geophys. Res. 113, Issue E12, CiteID E12006.
939 Mellon, M.T., 1996. Limits on the CO_2 content of the Martian polar deposits, Icarus 124, 268-
940 279.
941 Mellon, M.T., Feldman,W.C., Prettyman, T.H., 2004. The presence and stability of groundice
942 in the southern hemisphere of Mars, Icarus 169, 324–340.
943 Michalski, J. & Niles, P. B., 2011, Origin of Martian Sulfates and Interior Layered Deposits
944 (ILDs) in the Valles Marineris by atmospherically driven processes, EPSC-DPS Joint
945 Meeting 2011, 1752.
946 Miller, S.L., Smythe, W.D., 1970. Carbon Dioxide Clathrate In The Martian Ice Cap, Science
947 170, 531-533.
948 Morbidelli, A., Tsiganis, K., Crida, A., Levison, H., Gomes, R., 2007, Dynamics of the giant
949 planets of the solar system in the gaseous protoplanetary disk and their relationship to the
950 current orbital architecture, Astron. J. 134:1790-1798.
951 Moroz, V. I., 1998. Chemical composition of the atmosphere of Mars. Advances in Space
952 Research 22, 449-457.
953 Mousis, O., Lunine, J.I., Chassefière, E., Montmessin, F., Lakhlifi, A., Picaud, S., Petit, J.-M.,
954 Cordier, D, 2012. Mars cryosphere: A potential reservoir for heavy noble gases?, Icarus
955 218, 80-87.
956 Mousis, O., Chassefière, E., Lasue, J., Chevrier, V., Elwood Madden, L.E., Lakhlifi, A.,
957 Lunine, J.I., Montmessin, F., Picaud, S., Schmidt, F., Swindle, T.D., 2012. Volatile
958 trapping in Martian clathrates, Space Sci. Rev., in press, doi 10.1007/s11214-012-9942-9.

959 Mumma, M. J., Villanueva, G. L., Novak, R. E., Hewagama, T., Bonev, B. P., DiSanti, M. A.,
960 Mandell, A. M., Smith, D. M., 2009. Strong Release of Methane on Mars in Northern
961 Summer 2003, Science 323, 1041-1045.
962 Murchie, S.L., Mustard, J.F., Ehlmann, B.L., Milliken, R.E., Bishop, J.L., McKeown, N.K.,
963 Noe Dobrea, E.Z., Seelos, F.P., Buczkowski, D.L., Wiseman, S.M., Arvidson, R.E., Wray,
964 J.J., Swayze, G., Clark, R.N., Des Marais, D.J., McEwen, A.S., Bibring, J.P., 2009. A
965 synthesis of Martian aqueous mineralogy after 1 Mars year of observations from the Mars
966 Reconnaissance Orbiter, J. Geophys. Res. 114, E00D06, doi:10.1029/2009JE003342.
967 Niles, P.B., Catling, D.C., Berger, G., Chassefière, E., Ehlmann, B.L., Michalski, J.R.,
968 Morris, R., Ruff, S.W., Sutter, B. 2012. Geochemistry of Carbonates on Mars :
969 implications for climate history and nature of aqueous environments, Space Sci. Rev., in
970 press, doi 10.1007/s11214-012-9940-y.
971 Nummedal, D., Prior, D. B., 1981, Generation of Martian chaos and channels by debris flows,
972 Icarus 45, 77–86.
973 Ody, A., Poulet, F., Bibring, J.-P., Loiseau, D., Carter, J., Gondet, B., Langevin, Y., 2012.
974 Global investigation of olivine on Mars : insights into crust and mantle composition,
975 submitted to J. Geophys. Res. (in revision).
976 Owen, T., K. Biemann, D.R. Rushneck, J.E. Biller, D.W. Howarth, LaFleur, A.L. 1977. The
977 composition of the atmosphere at the surface of Mars. J. Geophys. Res. 82, 4635-4639.
978 Parrish, W.R., Prausnitz, J. M., 1972. Dissociation pressure of gas hydrates formed by gas
979 mixtures. Ind. Eng. Chem. Process Develop., 11, 26-35.
980 Pepin, R. O. 1991. On the origin and early evolution of terrestrial planet atmospheres and
981 meteoritic volatiles. Icarus 92, 2-79.
982 Pollack, J. B., Kasting, J.F., Richardson, F.M., Poliakoff, K., 1987. The Case for a Wet,
983 Warm Climate on Early Mars. Icarus. 71, 203-224.

Postawko, S. E., Kuhn, W. R., 1986. Effect of the greenhouse gases (CO_2, H_2O, SO_2) on Martian paleoclimate. Journal of Geophysical Research (Proc. Lunar Planet. Sci. Conf. 16th). 91, D431.

Quantin, C., Allemand, P., Mangold, N., Delacourt, C. 2004. Ages of Valles Marineris (Mars) landslides and implications for canyon history, Icarus 172, 2, 555- 572.

Rodriguez, J. A. P., Kargel, J., Crown, D. A., Bleamaster, L. F., Tanaka, K. L., Baker, V., Miyamoto, H., Dohm, J. M., Sasaki, S., Komatsu, G., 2006. Headward growth of chasmata by volatile outbursts, collapse, and drainage: Evidence from Ganges chaos, Mars, Geophys. Res. Lett. 33, Issue 18, CiteID L18203.

Segura, T.L., Toon, O.B., Colaprete, A., Zahnle, K. 2002. Environmental Effects of Large Impacts on Mars, Science 298, Issue 5600, 1977-1980.

Segura, T.L., Toon, O.B., Colaprete, A., 2008. Modeling the environmental effects of moderate-sized impacts on Mars, J. Geophys. Res. 113, Issue E11, CiteID E11007.

Sloan, E.D., 1998. Clathrate hydrates of natural gases. 2nd Ed. Marcel Decker, New York.

Sloan, E.D., Koh, C.A., 2007. Clathrate hydrates of natural gases. 3nd Ed. CRC Press.

Smith, D. E, Zuber, M. T., Frey, H. V., Garvin, J. B., Head, J. W., Muhleman, D. O., Pettengill, G. H., Phillips, R. J., Solomon, S. C., Zwally, H. J., Banerdt, W. B., Duxbury, T. C., Golombek, M. P., Lemoine, F. G., Neumann, G. A., Rowlands, D. D., Aharonson, O., Ford, P. G., Ivanov, A. B., Johnson, C. L., McGovern, P. J., Abshire, J. B., Afzal, R. S., Sun, X., 2001. Mars Orbiter Laser Altimeter: Experiment summary after the first year of global mapping of Mars, J. Geophys. Res. 106, E10, 23689-23722.

Squyres, S. W., Kasting, J. F., 1994. Early Mars: How Warm and How Wet? Science 265, Issue 5173, 744-749.

Squyres, S. W., Grotzinger, J. P., Arvidson, R. E., Bell, J. F., Calvin, W., Christensen, P. R., Clark, B. C., Crisp, J. A., Farrand, W. H., Herkenhoff, K. E., Johnson, J. R., Klingelhöfer, G., Knoll, A. H., McLennan, S. M., McSween, H. Y., Morris, R. V., Rice, J. W., Rieder,

R., Soderblom, L. A., 2004, In Situ Evidence for an Ancient Aqueous Environment at Meridiani Planum, Mars, Science 306, 1709-1714.

Tanaka, K. L., 1999, Debris-flow origin for the Simud/Tiu deposit on Mars, J. Geophys. Res. 104, 8637–8652.

Tian, F., Kasting, J.F., Solomon, S.C., 2009. Thermal escape of carbon from the early Martian atmosphere. Geophys. Res. Lett. 36, Issue 2, CiteID L02205.

Tian, F., Claire, M.W., Haqq-Misra, J. D., Smith, M., Crisp, D. C., Catling, D., Zahnle, K., Kasting, J. F., 2010. Photochemical and climate consequences of sulfur outgassing on early Mars. Earth and Planetary Science Letters. 295, 412-418.

Udachin, K.A. , Ratcliffe, C.I., Ripmeester, J.A. , 2002, Single Crystal Diffraction Studies of Structures I. II and H Hydrates: Structure. Cage Occupancy and Composition, Journal of Supra Molecular Chemistry 2, 405-408.

Van Berkum. J. G., Diepen. G. A. M., 1979, Phase equilibria in $SO_2 + H_2O$: the sulfur dioxide gas hydrate. two liquid phases. and the gas phase in the temperature range 273 to 400 K and at pressures up to 400 MPa, J. Chem. Thermodyn. 11., 317-334.

Von Stackelberg, M, 1949, Solid Gas Hydrates, Die Naturwissenschaften 36(12), 359-362.

Wilson, L., and J. W. Head III (2002), Tharsis-radial graben systems as the surface manifestation of plume-related dike intrusion complexes: Models andimplications, J. Geophys. Res. 107(E8), 5057, doi:10.1029/2001JE001593.

Wong, A.-S., Atreya, S. K., Encrenaz, Th, 2003, Chemical markers of possible hot spots on Mars, J. Geophys. Res. 110, E4, 5026, doi:10.1029/2002JE002003.

Wray, J.J., Murchie, S.L., Squyres, S.W., Seelos, F.P., Tornabene, L.L., 2011. Diverse aqueous environments on ancient Mars revealed in thesouthern Highlands, Geology 37, 11, 1043–1046, doi: 10.1130/G30331A.1.

Yasuda, K., Ohmura, R., 2008. Phase Equlibrium of Clathrate Hydrates Formed with Methane, Ethane, Propane or Carbon Dioxyde at temperatures below the Freezing Point of Water. J. Chem. Eng. Data 53, 2182-2188

Appendix A

A.1 Description of the statistical-thermodynamic model

Three main clathrate hydrate structures have been identified: SI, SII and SH. They differ by their crystallographic structure in which water is organized in a three dimensional network. It liberates internal cavities of different polyhedral types called 5^{12}, $5^{12}6^2$, $5^{12}6^4$, $4^3 5^6 6^3$ and $5^{12}6^8$ (e^f describes a polyhedron: e is the number of edges of the face, and f is the number of faces with e edge). In Table A1 are described more precisely the SI and SII structures, the major ones to be formed due to the composition of Martian gases. Table A1

In the case of clathrate hydrates in thermodynamic equilibrium, below the water freezing point, the equality of chemical potentials of water in the ice phase and in the hydrate phase can be written, by introducing a hypothetical reference state (phase β) corresponding to a hydrate with empty cavities:

$$\Delta\mu_w^{H-\beta} = \Delta\mu_w^{I-\beta}, \quad (1)$$

where $\Delta\mu_w^{H-\beta}$ and $\Delta\mu_w^{I-\beta}$ are the differences of the chemical potentials between water in hydrate (H) or ice (I) and water in the reference phase (β), respectively.

Modeling of $\Delta\mu_w^{H-\beta}$

$\Delta\mu_w^{H-\beta}$ is then determined from statistical thermodynamics whereas $\Delta\mu_w^{I-\beta}$ is determined by means of relations from classical thermodynamics that can be expressed as a function of the fugacity f_j of the gas j as:

$$\Delta\mu_w^{H-\beta} = RT\sum_i \nu_i \ln\left(1-\sum_j \theta_j^i\right) = RT\sum_i \nu_i \ln\left(1-\sum_j C_j^i f_j(T,P)\right) \quad (2)$$

where v_i is the number of cavities of type i, C_j^i is the Langmuir constant of component j in the cavity i describing the interaction potential between the encaged guest molecule and the surrounding water molecules, evaluated by assuming a spherically symmetrical cage and associated potential:

$$C_j^i = \frac{4\pi}{kT}\int_0^\infty \exp\left(-\frac{w(r)}{kT}\right) r^2 dr\,, \tag{3}$$

where w is the radial interaction potential between the guest molecule and the water molecules forming the structure. The interaction potential, when described by a Kihara model (Mckoy and Sinagoglu, 1963), can be expressed as:

$$w(r) = 2z\varepsilon\left[\frac{\sigma^{12}}{\overline{R}^{11} r}\left(\delta^{10} + \frac{a}{\overline{R}}\delta^{11}\right) - \frac{\sigma^{6}}{\overline{R}^{5} r}\left(\delta^{4} + \frac{a}{\overline{R}}\delta^{5}\right)\right] \tag{4}$$

$$\delta^N = \frac{1}{N}\left[\left(1 - r/\overline{R} - a/\overline{R}\right)^{-N} - \left(1 + r/\overline{R} - a/\overline{R}\right)^{-N}\right] \tag{5}$$

The gas parameters ε, σ and a are the Kihara parameters describing the potential we seek for and can be calculated from experimental data by fitting the model equations to corresponding hydrate equilibrium experimental data. The interaction potential takes into account the geometrical properties of the cavities (coordination number z and average mean radius $\overline{R}$, given in Table A1).

The equations that can be used to evaluate $\Delta\mu_w^{t-\beta}$, the difference in chemical potential between ice and the reference state T_0 = 273.15 K and the pressure P_0 = 1 bar are summarized in chapter 5 and in particular in Table 5.9 of Sloan and Koh (2008) and Table 4.3.1 of Herri et al (2011). The corresponding values of the reference state parameters used in the model are given in Table A2.

Equilibrium :

A simultaneous minimization of the three Kihara parameters (sigma, core radius and epsilon/k) on the clathrate hydrate model faces a high level of degeneracy, an issue amplified by the paucity of available equilibrium data in the sulfur dioxide case. In a rather well defined and measured system the degeneracy remains an issue (Herri et al., 2011). This is somehow already reflected in the distinct Kihara parameters deduced in the literature. Kihara parameters for pure substances can be evaluated from measurement of the viscosity, or can be calculated from the second virial coefficient, or from a combination of measurements (Tee et al , 1996). Also, they can be evaluated from Henry constants (Uno et al, 1975). The principle is to retrieve the Kihara parameters over experimental data with a limited number of pure substances. The authors propose a correlation to estimate the Kihara parameters for all kinds of gases. The optimization strategy we adopt to reduce the degeneracy is to set one of the parameters before to deduce the corresponding two others by minimization, as suggested in e.g. Mehta andSloan (1996). They propose to fix the Kihara *a* value. Based on the parameterization by Tee et al (1966) and Uno et al (1975) for SO_2, the core radius *a* value is estimated to lie close to *a*=0.75 Å, that we further set to explain the analysis performed.

Then, for a given set of Kihara parameters ε_j and σ_j, and a given temperature (resp. a given pressure), the calculated equilibrium pressure P_{calc} (resp. the calculated equilibrium temperature T_{calc}) corresponds to the value such as $\Delta\mu_w^{II-\beta} = \Delta\mu_w^{l-\beta}$. Then the calculated pressure and temperature are compared to the experimental ones $P_{\exp}$ and $T_{\exp}$ **,** and a deviation function can be defined as:

$$F(\varepsilon_j,\sigma_j)=\sum_{l=1}^{N}\left|\frac{P_{calc}}{P_{\exp}}-1\right|\rightarrow \min \text{ (resp. } F(\varepsilon_j,\sigma_j)=\sum_{l=1}^{N}\left|\frac{T_{calc}}{T_{\exp}}-1\right|\rightarrow \min \text{)} \qquad (6)$$

The summation is performed over all *N* data of the set.

In the work of Herri and Chassefière (2012), the Kihara parameters for CO_2 clathrate hydrate were retrieved with such a scheme, with ε/k=178.21K, *a*=0.6805Å and σ=2.873Å. By using the same method, the present work aims at retrieving the Kihara parameters for SO_2 hydrate.

A.2 Retrieving the SO_2 Kihara parameters

We focus on the value of *a*=0.75 Å, but the minimization was performed over a broader range of *a* values. Then, the ε and σ can be optimized from experimental results. Using the Tamman and Krige (1925) data, the minimized ε and σ values dependencies are shown in Fig. A1, following a valley of minima all satisfying the available experimental data. Using another core radius value would give rise to another satisfying correlation. With the limited data available, covering only the range of temperature from 261.15 K to 271.15 K, corresponding pressure and temperature SO_2 clathrate hydrate equilibria at lower temperatures are shown in Fig. A2 (in this case the core radius was explored over a larger range). Nevertheless, taking into account the regression uncertainties, significant constraints can be set in the Martian context as shown in the next section.

Captions for tables :

Table A1: Structure of SI and SII gas Hydrates

Table A2: Reference state parameters

Captions for figures :

Figure 1: Evolution of the cumulated amount of volcanically released sulfur in terms of SO_2 pressure (left vertical scale) and thickness of the corresponding sulfate mineral GEL (right vertical scale), assuming full conversion of sulfur into sulfate minerals. The "C&G" curve (dotted-dashed line) is obtained by multiplying by 10 the curve proposed in CG09 from a photogeological analysis of surface morphology (Greeley and Schneid, 1991). The two other curves are derived from CO_2 evolution curves proposed by Grott et al. (2011), as explained in the main text. These curves give the amount of CO_2 released from mantle carbon and don't include a possible contribution of superficial carbon (e.g. carbonates) to the volcanic CO_2.

Figure 2: Mean surface temperature as a function of the CO_2 pressure for SO_2 mixing ratios of 0, 1, 10 and 100 ppm show the cooling effect of SO_2 aerosols at p_{CO2} = 3 bar and mixing ratios of SO_2 of 1 ppm and 10 ppm. The equilibrium temperatures of CO_2 clathrate hydrate, and CO_2 ice, are plotted as a function of CO_2 pressure (from Mousis et al., 2012).

Figure 3: Ratio of concentration in mixed SO_2-CO_2 clathrate hydrate with respect to gas phase one as a function of temperature using the different constrained extrapolated SO_2 Kihara parameters. Initial SO_2 concentrations are 0.1 ppm (circles, blue curves) and 1000 ppm (triangles, red curves), covering most of the expected range for Martian conditions.

Figure 4: Surface temperature as a function the SO_2 mixing ratio for different values of the CO_2 partial pressure : 3 bar, 1.5 bar, 1 bar, 0.5 bar. The black triangles correspond to the SO_2 mixing ratio for which the temperature is equal to the CO_2 clathrate equilibrium temperature.

Figure 5: Equilibrium SO_2 mixing ratio as a function of CO_2 pressure. The lava volumes required to give rise to the corresponding SO_2 mixing ratio, calculated by using the same conversion factor as in Johnson et al. (2008), are indicated on the figure.

Figure 6: CO_2 evolution profile scaled on the Chassefière and Leblanc (2011a) profile to fit a 2 bar value at 3.8 Gyr b.p. (solid line). Blue rectangles with dotted lines and blue "average" dotted curve represent the evolution of the crust production rate derived from photogeological analysis (Greeley and Schneid, 1991). The chronology of clays, sulfates and ferric oxides proposed by Bibring et al. (2006) is shown at the top. The vertical grey band corresponds to the time interval when volcanic activity was significant according to Greeley and Schneid estimates.

Figure 7: Schematic representation of sulfur and CO_2 reservoir during the Noachian and Hesperian period. The total volatile surface/atmosphere CO_2 reservoir is decreasing due to thermal escape and possible formation of carbonates in the subsurface, from an initial budget ~100 bar. After magma ocean crystallization, CO_2 and water condense in form of clathrate (15 bar of CO_2 at maximum can be stored in form of clathrate when reacting with the total Martian water content of 1000 m GEL). After volcanic release of S, atmospheric SO_2 is systematically enriched in the condensating clathrate, triggered either by climatic changes or by global cooling due to aerosol formation. The CO_2 clathrate acts as an atmospheric buffer when the atmospheric pressure reaches 2 bar. After the complete consumption of CO_2 clathrate, the atmospheric pressure can drop below 2 bar and massive release of SO_2 from the clathrate induces the condensation of aerosols and precipitation as a Mars-wide sulfate layer (50 m represent the total SO_2 outgassed from Tharsis formation). This scenario represents the equilibrium state of surface/atmosphere but significant departure may have happened due to large impacts.

Figure 8: Mole fraction of volatiles encaged in clathrates calculated as a function of the surface pressure of CO_2 in the cases of, from top to bottom, SO_2 atmospheric abundances equal to 10^{-3}, 1 and 10^3 ppm.

Figure A1: Pearson's chi square test contour plot of the minimized ε/k versus σ for SO_2 Kihara parameters, with core radius a fixed at 0.75Å. Contour levels are spaced in powers of 3 of the best-regressed value. Pressure and temperature equilibrium data for SO_2 hydrate are taken from Tamman and Krige (1925)

Figure A2: Range of pressure and temperature extrapolated equilibrium for SO_2 clathrate hydrate using our model (small dots, colored range). The input Kihara parameters are obtained in the 3D $\{\varepsilon/k, \sigma, a\}$ parameter space regression on experimental data by setting the core radius in the $a \in [0.55,0.95]$ range, then regressing the degenerate Kihara parameters as shown in Fig. 3. Original data from Tamman and Krige (1925) (large circle) are displayed as well as water phase diagram limits.

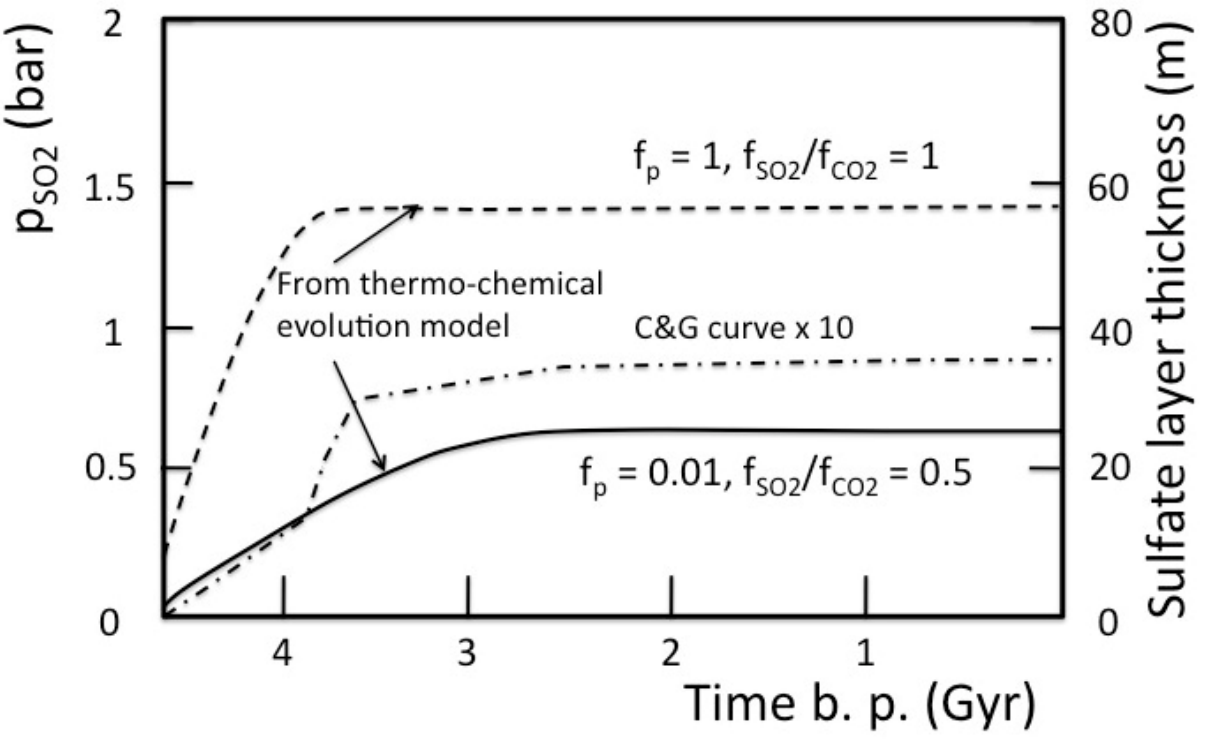

Figure 1

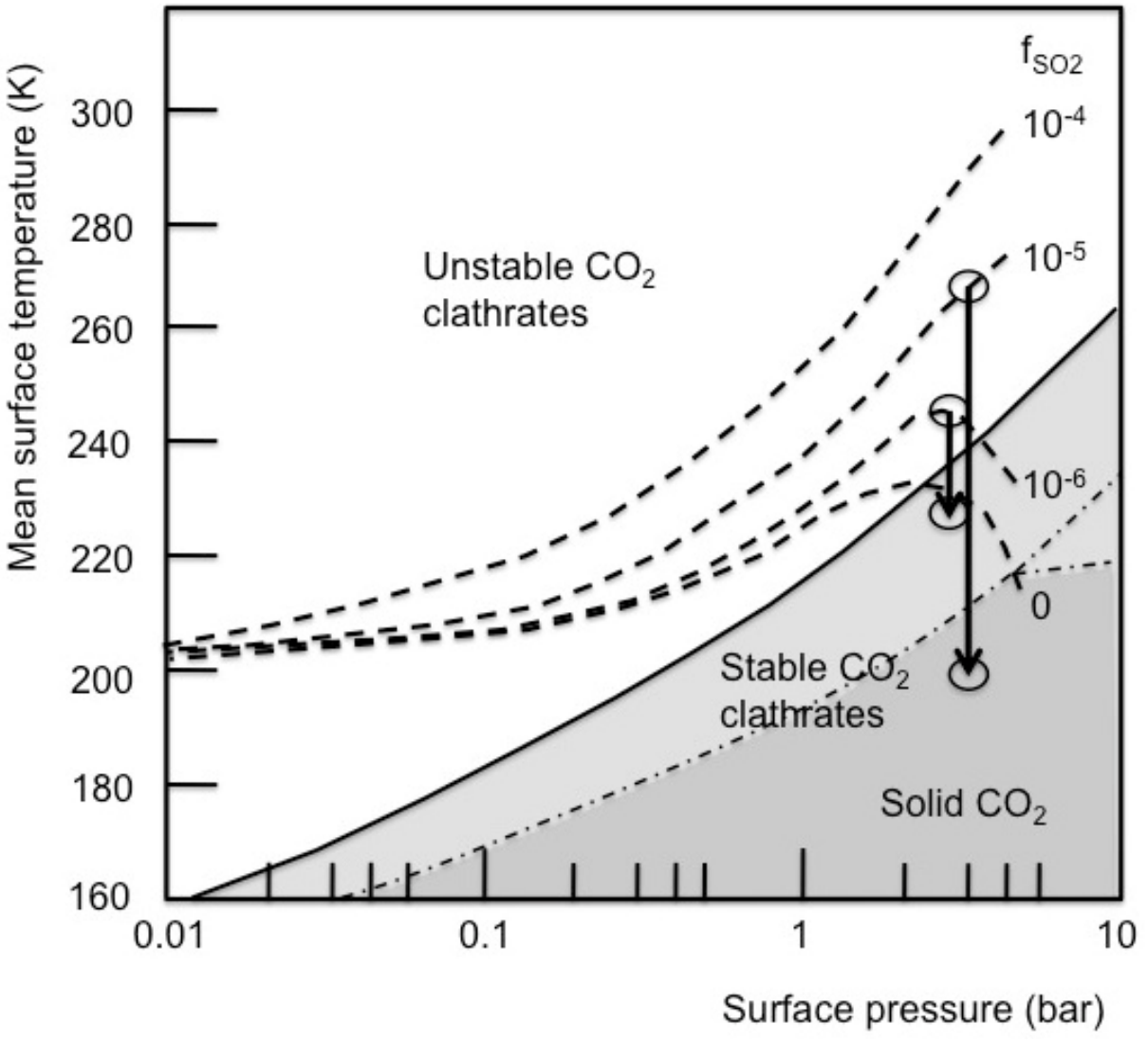

Figure 2

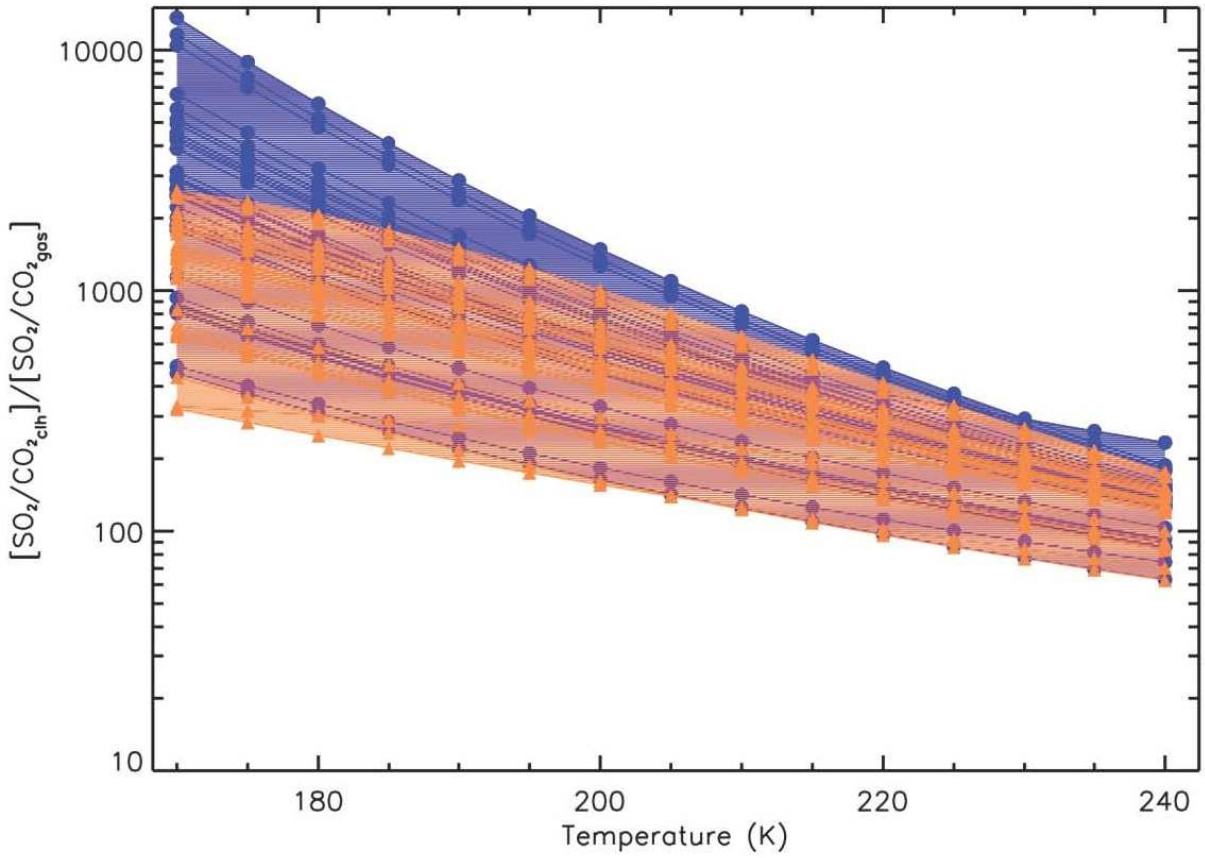

Figure 3

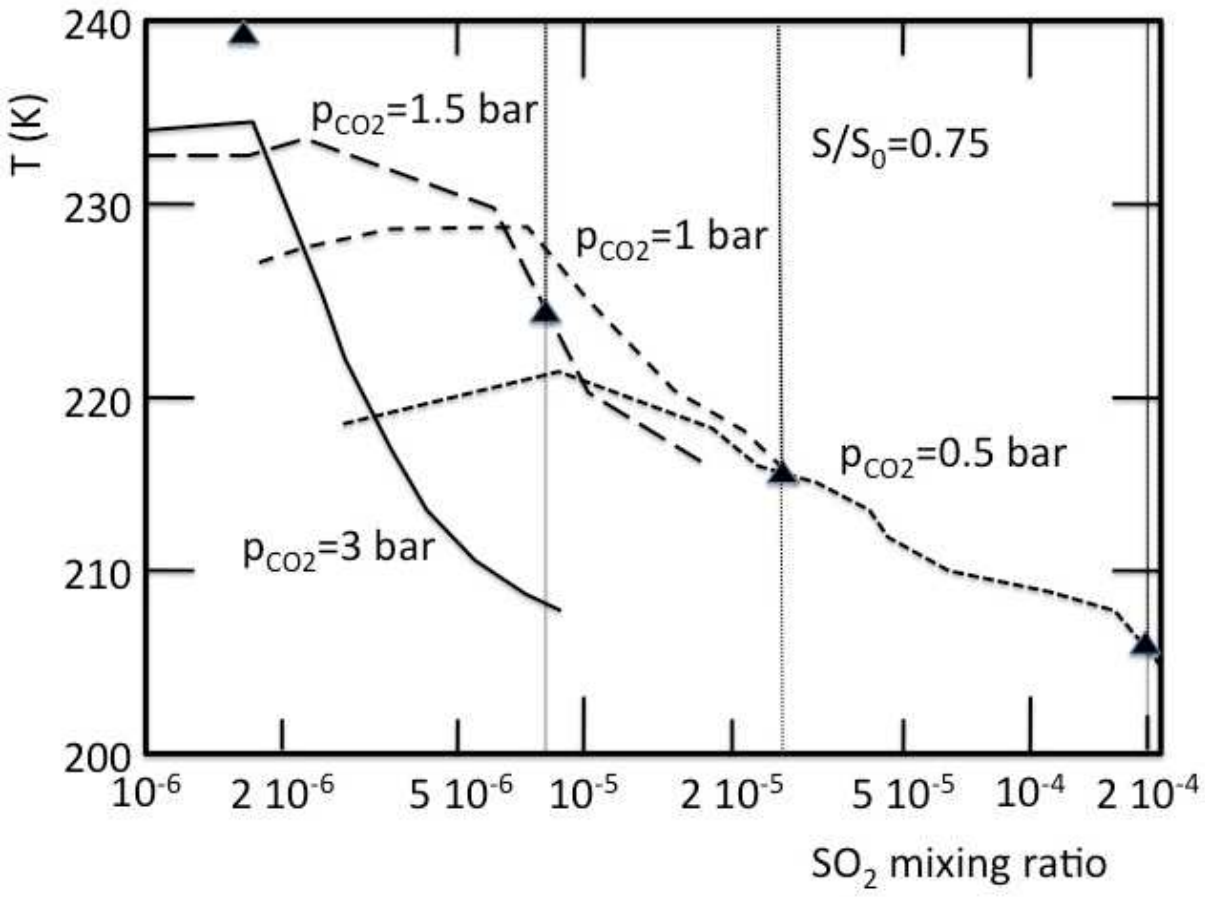

Figure 4

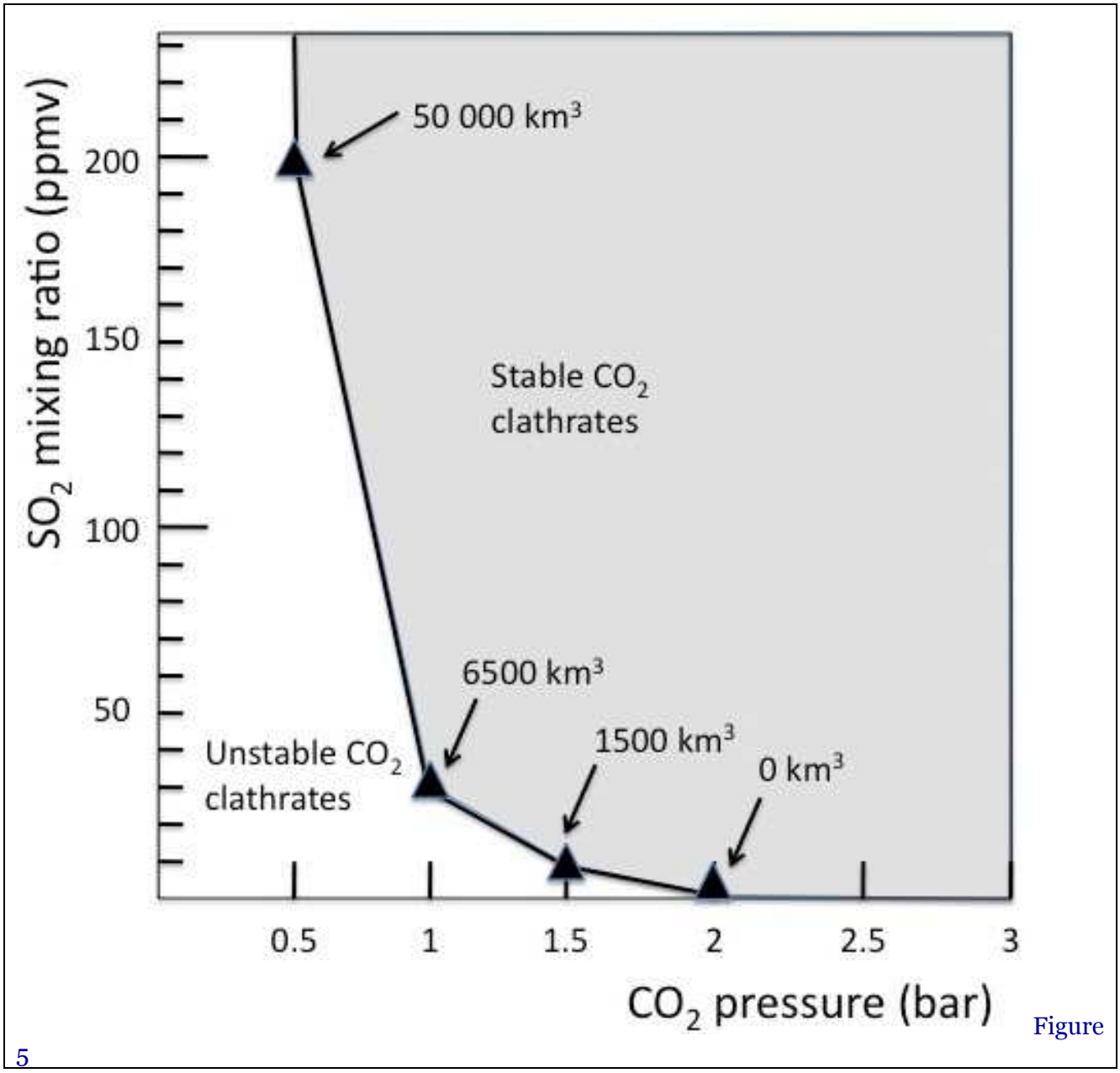
50 000 km³
Stable CO₂ clathrates
6500 km³
1500 km³
0 km³
Unstable CO₂ clathrates
SO₂ mixing ratio (ppmv)
200
150
100
50
0.5
1
1.5
2
2.5
3
CO₂ pressure (bar)

Figure 5

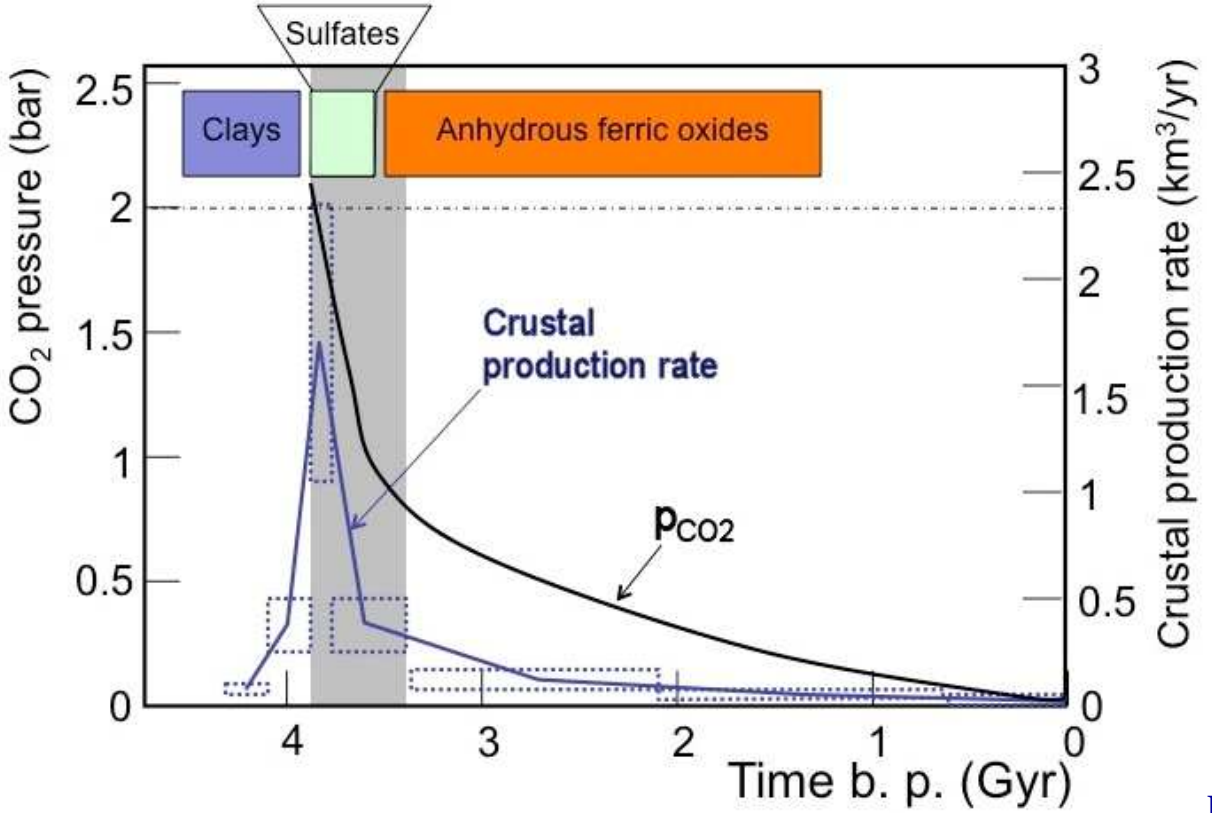

Figure 6

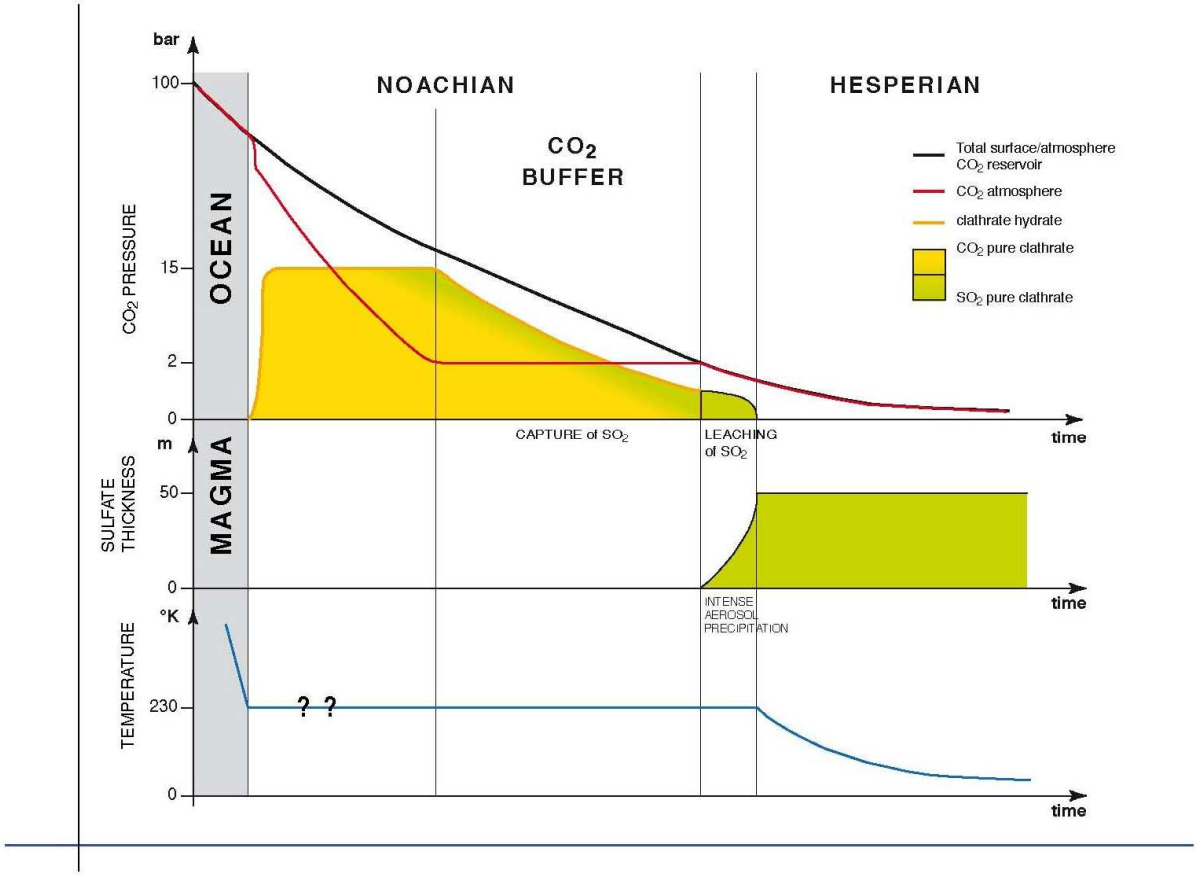

Figure 7

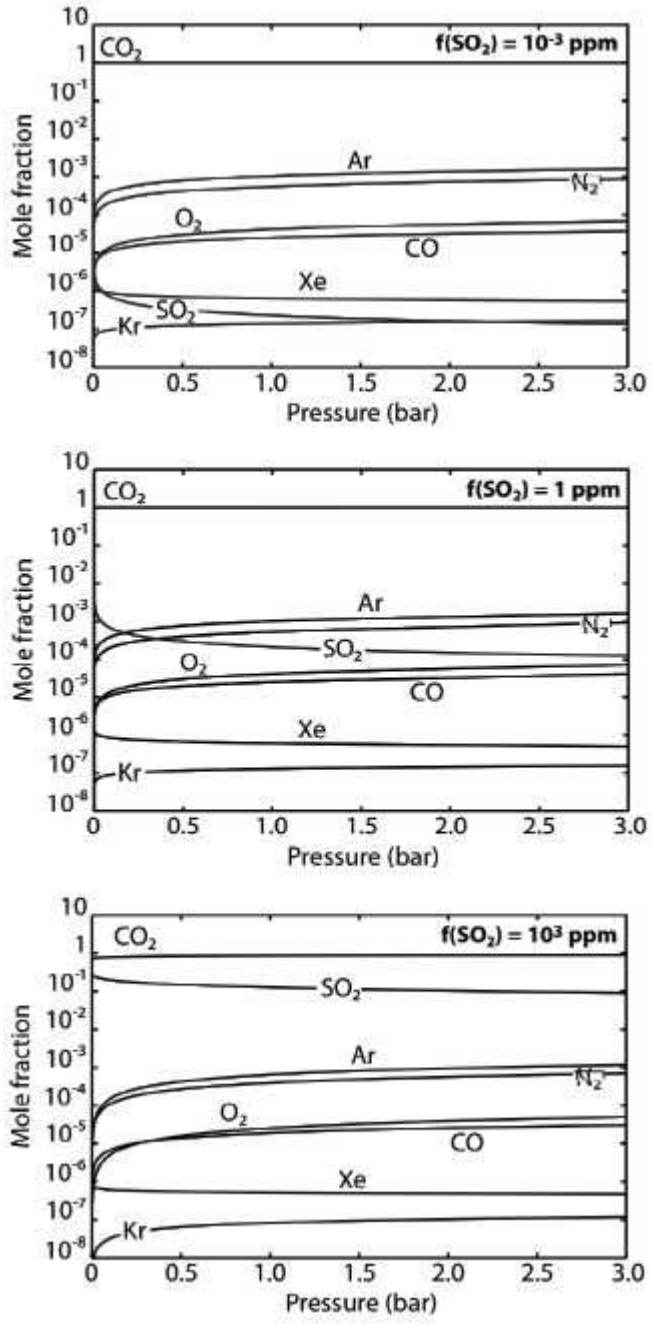
CO2
f(SO2) = 10-3 ppm
Ar
N2
O2
CO
Xe
SO2
Kr
Mole fraction
Pressure (bar)
CO2
f(SO2) = 1 ppm
Ar
N2
SO2
O2
CO
Xe
Kr
Mole fraction
Pressure (bar)
CO2
f(SO2) = 10³ ppm
SO2
Ar
N2
O2
CO
Xe
Kr
Mole fraction
Pressure (bar)

Figure 8

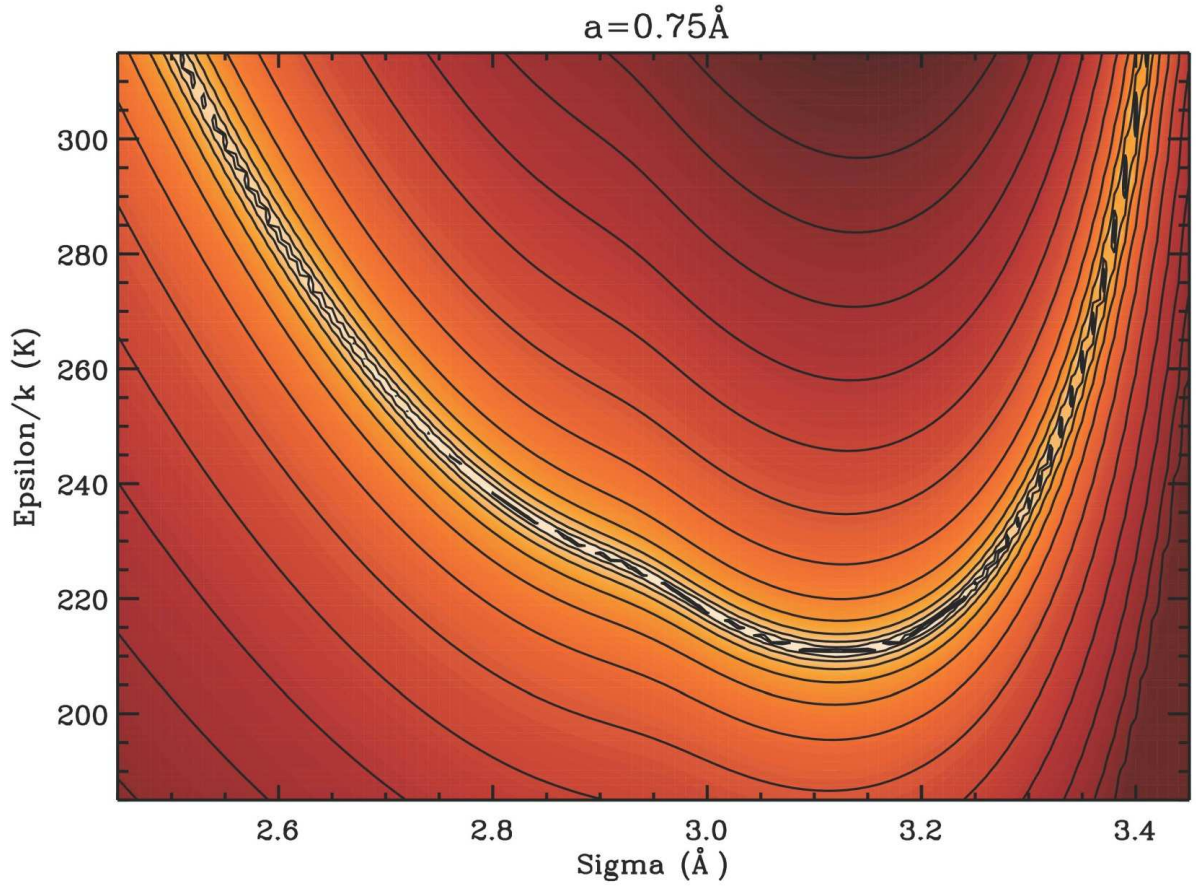

Figure A1

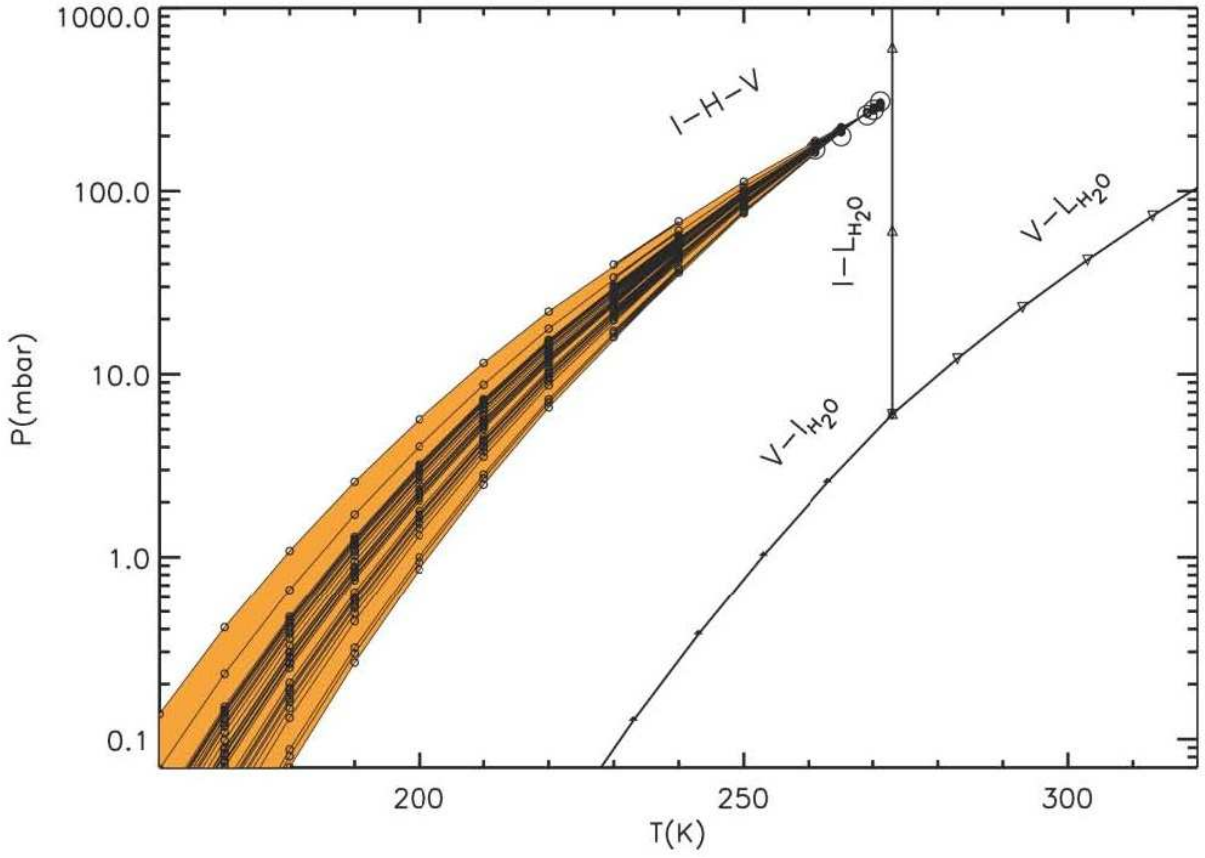

Figure A2